# Aluminum Effects in the Syndiospecific Copolymerization of Styrene with Ethylene by Cationic Fluorenyl Scandium Alkyl Catalysts

Xiaofang Li,*,[†] Xiaoying Wang,[†] Xin Tong,[†] Hongxia Zhang,[‡] Yuanyuan Chen,[†] Ying Liu,[†] Hui Liu,[†] Xiaojie Wang,[†] Masayoshi Nishiura,[‡] Huan He,[†] Zhenguo Lin,[†] Shaowen Zhang,*,[†] and Zhaomin Hou*,[‡]

[†]Key Laboratory of Cluster Science of Ministry of Education, School of Chemistry, Beijing Institute of Technology, 5 South Zhongguancun Street, Haidian District, Beijing 100081, People's Republic of China

[‡]Organometallic Chemistry Laboratory and Advanced Catalyst Research Team, RIKEN Advanced Science Institute, Hirosawa 2-1, Wako, Saitama 351-0198, Japan

Ⓢ *Supporting Information*

ABSTRACT: A series of half-sandwich fluorenyl (Flu′) scandium dialkyl complexes Flu′Sc(CH$_2$SiMe$_3$)$_2$(THF)$_n$ (**1**, Flu′ = C$_{13}$H$_9$, n = 1; **2**, Flu′ = 2,7-^{t}Bu$_2$C$_{13}$H$_7$, n = 1; **3**, Flu′ = 9-SiMe$_3$C$_{13}$H$_8$, n = 1; **4**, Flu′ = 2,7-^{t}Bu$_2$-9-SiMe$_3$C$_{13}$H$_6$, n = 1; **5**, Flu′ = 9-CH$_2$CH$_2$NMe$_2$C$_{13}$H$_8$, n = 0; **6**, Flu′ = 2,7-^{t}Bu$_2$-9-CH$_2$CH$_2$NMe$_2$C$_{13}$H$_6$, n = 0) have been synthesized and structurally characterized. In comparison with the well-known cyclopentadienyl-ligated scandium catalyst system [(C$_5$Me$_4$SiMe$_3$)Sc-(CH$_2$SiMe$_3$)$_2$(THF)]/[Ph$_3$C][B(C$_6$F$_5$)$_4$], the analogous combinations of the fluorenyl-ligated, THF-containing complexes **1–4** with [Ph$_3$C][B(C$_6$F$_5$)$_4$] show relatively low activities, albeit with similar syndioselectivities for styrene polymerization and styrene–ethylene copolymerization. However, on treatment with 15 equiv of Al^{i}Bu$_3$, the **1–4**/[Ph$_3$C][B(C$_6$F$_5$)$_4$] combinations show a dramatic increase in catalytic activity without changes in the stereoselectivity. In contrast, the combinations of complexes **5** and **6**, which have an amino group attached to the fluorenyl ring and intramolecularly bonded to the metal center, exhibit very low activity, no matter whether or not Al^{i}Bu$_3$ is present, affording syndiotactic polystyrenes with broad molecular weight distributions. The DFT calculations of the activation mechanism by using the representative catalysts suggest that Al^{i}Bu$_3$ can capture the THF molecule from the catalyst precursors **1–4** at first, and then the new, THF-free cationic half-sandwich scandium active species [Flu′Sc(CH$_2$SiMe$_3$)][B(C$_6$F$_5$)$_4$] with less steric hindrance around the metal center is generated in the presence of an activator such as [Ph$_3$C][B(C$_6$F$_5$)$_4$]. The DFT calculations on the syndioselectivity of styrene (co)polymerization catalyzed by [Flu′Sc(CH$_2$SiMe$_3$)][B(C$_6$F$_5$)$_4$] have also been carried out, thus shedding new light on the mechanistic aspects of the (co)polymerization processes.
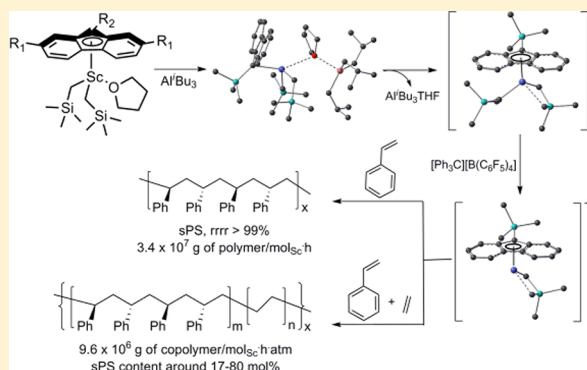
INTRODUCTION

The clear identification of cationic active species in well-defined catalyst systems that consist of metal alkyls and borate/borane-based cation generating agents has significantly advanced the mechanistic understanding of olefin coordination polymerization processes.[1] Because of the high sensitivity of these highly electrophilic cationic species toward trace impurities, the extra addition of a small amount of aluminum alkyls (AlR$_3$) is usually beneficial.[2] In some cases, however, the presence of AlR$_3$ not only changes the catalytic activity but also switches the catalytic performance of the binary cationic catalyst in the olefin (co)polymerization, suggesting that some uncertain reaction occurring during the activation processes induces a change of active species. What is the special function of AlR$_3$ in such ternary cationic catalysts? This question has attracted much attention.

In general, AlR$_3$ has a 3-fold effect in olefin (co)-polymerization: scavenging impurities, transforming (alkylating and reducing) the cationic species, and acting as a chain transfer agent.[1] However, the Lewis acid properties of AlR$_3$ other than these effects have also been extensively investigated. It is found that AlR$_3$, especially AlMe$_3$, can react with a catalyst precursor to form a heterobinuclear metal–alkylaluminum complex. For example, the heterobinuclear cations [Cp′$_2$M(μ-Me)$_2$AlMe$_2$]-[B(C$_6$F$_5$)$_4$] have been identified by NMR spectroscopy as the predominant species in the ternary group 4 metallocene catalyst system Cp′$_2$MMe$_2$/[Ph$_3$C][B(C$_6$F$_5$)$_4$]/AlMe$_3$.[3] In the case of a ternary group 3 metallocene catalyst such as [(C$_5$Me$_5$)$_2$LnR/[Ph$_3$C][B(C$_6$F$_5$)$_4$]/AlMe$_3$, the heteromultimetallic complex (C$_5$Me$_5$)$_2$Ln[(μ-Me)AlMe$_2$(μ-Me)]$_2$Ln(C$_5$Me$_5$)$_2$ (Ln = Sm, Pr, Nd, Gd) was first formed by the reaction of the metallocene alkyl precursor with AlMe$_3$, which after activation by [Ph$_3$C]-

$[B(C_6F_5)_4]$ showed excellent cis-1,4-selectivity (up to 99%) for the polymerization of butadiene.[4] In 2008, Hou et al. reported that the regio- and stereoselectivity of isoprene polymerization by the non-metallocene yttrium catalyst system $(NCN^{dipp})Y(o\text{-}CH_2C_6H_4NMe_2)_2/[Ph_3C][B(C_6F_5)_4]$ could be switched from 3,4-isospecific to cis-1,4-selective simply by adding 10 equiv of $AlMe_3$.[5] The heterotrinuclear intermediate $[(NCN^{dipp})Y\{(\mu\text{-}Me)_2AlMe_2\}_2]$ was isolated and characterized by X-ray diffraction. Anwander and co-workers reported that the heterotrinuclear complexes $(C_5Me_5)Ln(AlMe_4)_2$ promoted living trans-1,4-polymerization of isoprene in the presence of $[Ph_3C][B(C_6F_5)_4]$.[6] In comparison to the $AlMe_3$-involved systems, analogous heterometallic isobutylaluminum ternary catalysts containing Al^iBu_3 (TIBA) have been much less extensively explored. In 2005, Evans et al. reported that $[(C_5Me_5)_2Sm(\mu\text{-}O_2CPh)]_2$ reacted with Al^iBu_3 to form the mixed bridge samarium/aluminum complex $[(C_5Me_5)_2Sm(\mu\text{-}O_2CPh)(\mu\text{-}^iBu)Al(^iBu)_2]$, which worked as a catalyst precursor for diene polymerization.[7] In 2008, Cui and co-workers observed formation of the scandium–isobutylaluminate ion pair $[(NPN^{Ph})Sc(\mu\text{-}CH_2SiMe_3)Al^iBu_2(\mu\text{-}CH_2CH(CH_3)_2)][B(C_6F_5)_4]$ by NMR spectroscopy in the reaction of $(NPN^{Ph})Sc(CH_2SiMe_3)_2(THF)$ with $[PhNHMe_2][B(C_6F_5)_4]$.[8] Hou and co-workers found that, unlike the case for $AlMe_3$, addition of Al^iBu_3 to the $(NCN^{dipp})Y(o\text{-}CH_2C_6H_4NMe_2)_2/[Ph_3C][B(C_6F_5)_4]$ catalyst system did not show significant influence on the selectivity of isoprene polymerization.[5] Generally, it is thought that the $\mu\text{-}^iBu$ species are more difficult to form because the stability of the μ-alkyl complexes decreases rapidly with increasing bulk of the alkyl group.[3g] Therefore, the truly active species responsible for the olefin (co)polymerization in ternary catalyst systems composed of metal alkyl/activator/Al^iBu_3 have been the subjects of considerable debate. The elucidation of the activation mechanism and the special function of Al^iBu_3 in some ternary cationic catalytic systems still remains a challenge.

Hou and co-workers also reported that binary systems composed of a half-sandwich scandium dialkyl complex such as $(C_5Me_4SiMe_3)Sc(CH_2SiMe_3)_2(THF)$ and 1 equiv of a borate compound such as $[Ph_3C][B(C_6F_5)_4]$ can serve as highly efficient catalysts for the (co)polymerization of a wide range of olefin monomers, such as syndiospecific polymerization of styrene, syndiospecific copolymerization of styrene with ethylene or isoprene, alternating and random copolymerization of isoprene with ethylene, alternating copolymerization of norbornene (or dicyclopentadiene) with ethylene, terpolymerization of norbornene (or dicyclopentadiene), ethylene, and styrene, and copolymerization of ethylene and unconjugated dienes.[9] In many of these reactions, the THF-free aminobenzyl complex $(C_5Me_4SiMe_3)Sc(CH_2C_6H_3NMe_2\text{-}o)_2$ showed higher activity and behaved differently in comparison to the THF-containing complex $(C_5Me_4SiMe_3)Sc(CH_2SiMe_3)_2(THF)$.[9f,q,r] Okuda and Tritto reported that the ternary catalyst $(C_5Me_4SiMe_3)Sc(CH_2SiMe_3)_2(THF)/[Ph_3C][B(C_6F_5)_4]/Al^iBu_3$ showed different behaviors in comparison to the binary catalyst $(C_5Me_4SiMe_3)Sc(CH_2SiMe_3)_2(THF)/[Ph_3C][B(C_6F_5)_4]$ in the copolymerization of ethylene with norbornene;[10] the former produced more norbornene–norbornene sequences in the resulting ethylene–norbornene copolymers. This difference might be due to possible abstraction of the THF ligand from the Sc ion by Al^iBu_3 to generate a THF-free active species in the ternary system.[10f]

We report here a new series of binary and ternary catalysts composed of half-sandwich scandium alkyl complexes bearing various substituted fluorenyl ligands for the polymerization and copolymerization of styrene and ethylene.[11] To gain a better insight into the Al^iBu_3 effect and the mechanism of the syndiospecific styrene (co)polymerization, thorough DFT studies have also been carried out.

RESULTS AND DISCUSSION

Synthesis and Structure of Half-Sandwich Fluorenyl Scandium Dialkyl Complex. The one-pot metathesis reaction of $ScCl_3(THF)_3$ with 1 equiv of the lithium salt of the substituted fluorenyl ligand followed by addition of 2 equiv of $LiCH_2SiMe_3$ in THF at 25 °C afforded the corresponding half-sandwich fluorenyl scandium dialkyl complexes $(Flu')Sc(CH_2SiMe_3)_2(THF)_n$ (**1**, Flu' = $C_{13}H_9$, $n = 1$; **2**, Flu' = $2,7\text{-}^tBu_2\text{-}C_{13}H_7$, $n = 1$; **3**, Flu' = $9\text{-}SiMe_3\text{-}C_{13}H_8$, $n = 1$; **4**, Flu' = $2,7\text{-}^tBu_2\text{-}9\text{-}SiMe_3\text{-}C_{13}H_6$, $n = 1$; **5**, Flu' = $9\text{-}CH_2CH_2NMe_2\text{-}C_{13}H_8$, $n = 0$; **6**, Flu' = $2,7\text{-}^tBu_2\text{-}9\text{-}CH_2CH_2NMe_2\text{-}C_{13}H_6$, $n = 0$) (Scheme 1). Extraction and crystallization from hexane at −30

Scheme 1. Synthesis of Half-Sandwich Fluorenyl Scandium Complexes
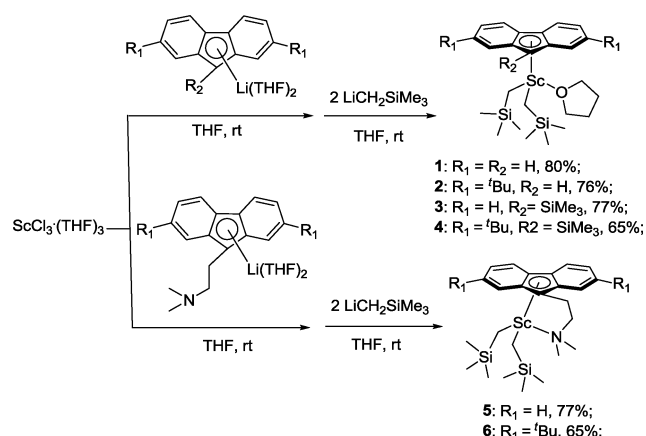
°C provided these complexes as crystals in good yields (65−80%). When complex **4** was extracted and crystallized by using a toluene/hexane solvent mixture, the chloride-bridged hetero-binuclear complex $(2,7\text{-}^tBu_2\text{-}9\text{-}SiMe_3C_{13}H_6)Sc(CH_2SiMe_3)_2(\mu\text{-}Cl)Li(THF)_3$ (**7**) was also obtained, probably due to the greater solubility of $ClLi(THF)_3$ in toluene than in hexane, increasing the coordination possibility of $ClLi(THF)_3$ with the metal center instead of THF solvent (Scheme 2).

Complexes **1**−**6** were fully characterized by elemental analysis, NMR spectroscopy, and single-crystal X-ray diffraction studies for **3**−**7**. The ORTEP drawings of **3**−**7** are shown in Figure 1. Their selected bond lengths and angles are summarized in Table 1. Despite the large differences in steric hindrance and electron density of the fluorenyl ligands in these complexes, the

Scheme 2. Synthesis of a Half-Sandwich Fluorenyl Scandium−Lithium Heterobinuclear Complex

7: 40%
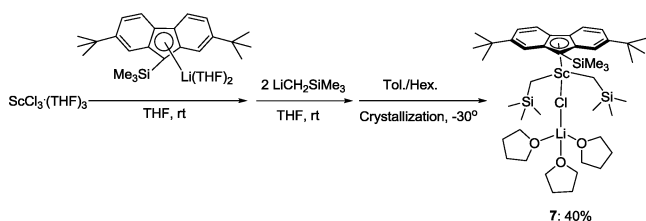
Figure 1. ORTEP drawings of **3−7** with thermal ellipsoids at 30% probability. Hydrogen atoms have been omitted for clarity.

Table 1. Selected Bond Distances (Å) and Angles (deg) of Complexes 3−7

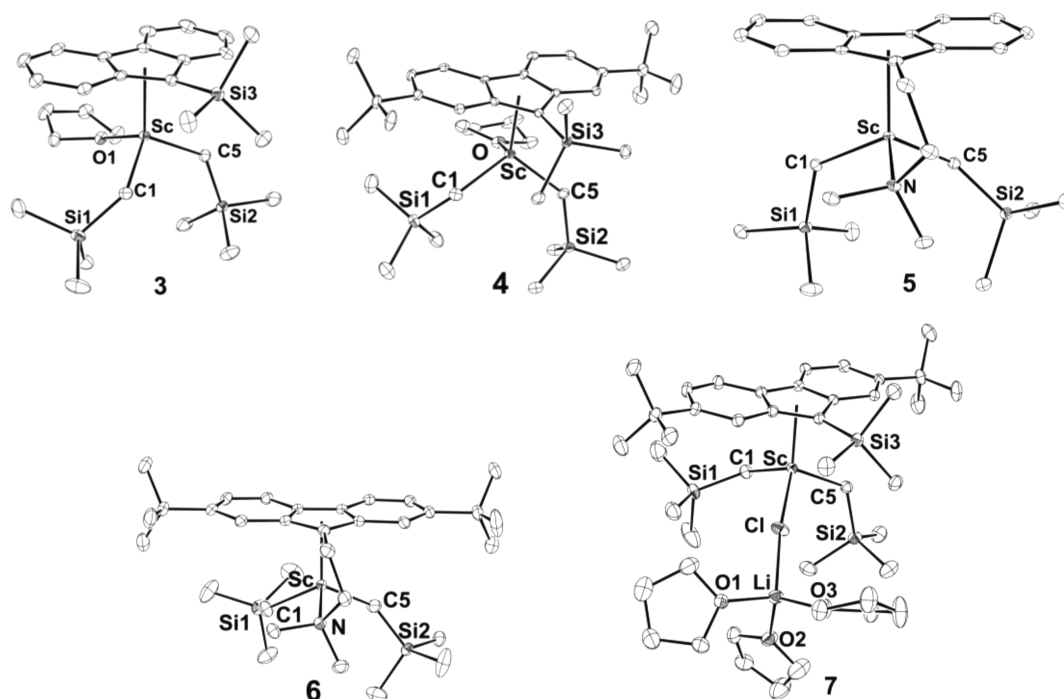|	3	4	5	6	7
Sc−Flu$_{av}$	2.583(2)	2.560(4)	2.555(2)	2.544(3)	2.582(3)
Sc−C1	2.201(2)	2.196(4)	2.211(2)	2.200(2)	2.221(3)
Sc−C5	2.213(2)	2.198(4)	2.199(2)	2.198(2)	2.215(4)
Sc−O/N/Cl	2.156(1)	2.146(3)	2.288(2)	2.307(2)	2.431(1)
O/N−Sc−C1	107.15(5)	104.81(13)	106.70(6)	100.49(8)	107.52(10)
O/N−Sc−C5	98.28(5)	98.14(14)	108.91(6)	108.10(8)	103.64(10)
C5−Sc−C1	106.19(6)	108.04(16)	103.75(7)	107.55(10)	98.62(14)
Si1−C1−Sc	130.03(9)	131.2(2)	129.82(10)	125.45(12)	130.82(19)
Si2−C5−Sc	132.99(8)	133.3(2)	140.36(10)	142.45(13)	125.44(18)
Sc-Flu$_{Cent(1)}$	2.274	2.265	2.248	2.188	2.275
Flu$_{Cent(1)}$−Sc−O/N/Cl	109.6	108.5	102.1	115.5	118.2
Flu$_{Cent(1)}$−Sc−C1	117.6	122.6	116.5	115.3	112.4
Flu$_{Cent(1)}$−Sc−C5	116.0	112.7	118.3	117.2	114.3

complexes **1−7** adopt a similar overall structure, in which the Sc metal center is bound to one fluorenyl unit, two alkyls, and one Lewis base. The monodentate fluorenyl complexes **1−4** contain a THF molecule as a Lewis base, while in complexes **5** and **6** having bidentate fluorenyl ligands, the intramolecular coordination of a nitrogen heteroatom in the side arm to the scandium center instead of the THF solvent molecule. However, ClLi(THF)$_3$ serves as the Lewis base in complex **7**. The Sc−Cp$'_{av}$ bond distances as well as the Sc−CH$_2$SiMe$_3$ bond distances in **3−7** are comparable among each other (Table 1) and are in the normal bond distance ranges reported previously for related complexes.[9] The chelating Sc−Cl(ClLi(THF)$_3$) bond distance in **7** (2.431(1) Å) is much longer than those of the Sc−O(THF) or Sc−N(NMe$_2$) found in **3−6** (2.146(3)−2.307(2) Å). In comparison, the Sc−N bond distances in **5** and **6** (2.288(2)−2.307(2) Å) are slightly longer than those of the Sc−O in **3** and **4** (2.146(3)−2.156(1) Å). The Sc−Flu$_{Cent(1)}$ bond distance decreases in the order **3** > **4** > **5** > **6**, perhaps due to the different coordination modes and the increasingly electron donating substituents on the fluorenyl ligands. The two

CH$_2$SiMe$_3$ groups in **3−7** both adopt a prone fashion,[12] similar to those of (C$_5$Me$_4$SiMe$_3$)Sc(CH$_2$SiMe$_3$)$_2$ (THF) (**8**),[9] suggesting the large steric hindrances of these substituted fluorenyl ligands. Differences in the coordination orientation of the Lewis base were observed among **3−7**, possibly as a result of the steric influence of the fluorenyl ligands. In **3**, **4**, and **7**, the THF ring plane is oriented almost parallel toward the Flu$'$ ring plane (Figure 1). In the case of **5** and **6**, the CH$_2$CH$_2$NMe$_2$ group adopts a vertical orientation to the fluorenyl ring. The correlation of the steric hindrances and the electron densities of these complexes and their activities and selectivities in the styrene (co)polymerization reaction are described below.

All complexes **1−7** are soluble in common organic solvents such as THF, toluene, and hexane and give well-resolved ^{1}H and ^{13}C NMR spectra in C$_6$D$_6$, without ligand redistribution being observed. Complexes **1** and **2** each show one singlet for the methylene protons of the two CH$_2$SiMe$_3$ groups at −0.11 and −0.06 ppm, respectively. In contrast, the methylene protons of the two CH$_2$SiMe$_3$ groups in **3** and **4** afford two doublets (**3**, −0.41 (d, 2H, J = 11.2 Hz), −0.25 ppm (d, 2H, J = 11.6 Hz); **4**,

Table 2. Syndiospecific Styrene Polymerization by Fluo′Sc(CH$_2$SiMe$_3$)$_2$(THF)$_n$/Activator/Al^{i}Bu$_3$ Catalytic Systems[a]
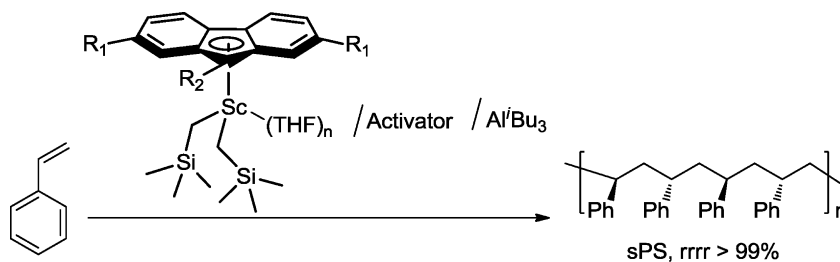
entry	compd	act.[b]	[Al]/[Sc]	[M]/[Sc]	t (min)	yield (%)	act.[c]	sPS[d]	M_n^e (×10^4)	M_w/M_n^e	T_m^f (°C)
1	1	A	15	2500	60	80	208	>99	43	3.77	268
2	2	A	15	2500	1	100	≥15623	>99	13	3.05	268
3	2	A	15	5500	1	100	≥34370	>99	12	4.60	267
4	2	A	15	6000	1	68	25496	>99	16	3.97	274
5	2	B	15	6000	1	71	26621	>99	20	4.45	267
6	2	C	15	6000	1	2	750	>99	6	5.93	272
7	3	A		500	1	88	2750	>99	7	1.97	271
8	3	A		2500	1	20	3125	>99	9	1.62	273
9	3	A	2	500	1	90	2812	>99	34	1.31	274
10	3	A	10	500	1	100	≥3125	>99	8	1.83	272
11	3	A	15	500	1	100	≥3125	>99	8	1.89	271
12	3	A	15	700	1	100	≥4374	>99	9	2.36	272
13	3	A	15	1000	1	100	≥6249	>99	13	2.22	272
14	3	A	15	1500	1	100	≥9374	>99	12	2.33	273
15	3	A	15	2000	1	100	≥12498	>99	19	2.56	273
16	3	A	15	2500	1	100	≥15623	>99	30	2.48	273
17	3	A	15	4000	1	100	≥24996	>99	78	2.40	273
18	3	A	15	5000	1	100	≥31245	>99	73	2.10	271
19	3	A	15	5500	1	100	≥34370	>99	67	2.33	272
20	3	A	15	6000	1	87	32620	>99	66	2.50	271
21	3	B	15	6000	1	90	33745	>99	63	4.05	272
22	3	C	15	6000	1	15	844	>99	16	2.01	272
23	4	A	15	2500	1	100	≥15623	>99	32	2.97	271
24	4	A	15	5500	1	100	≥34370	>99	64	4.13	274
25	4	A	15	6000	1	79	29620	>99	50	3.03	274
26	4	B	15	6000	1	83	31120	>99	55	2.38	269
27	4	C	15	6000	1	10	3749	>99	11	1.65	274
28	5	A		2500	300	13	7	>99	13	3.05	269
29	5	A	15	2500	300	25	13	>99	77, 1	1.81, 1.39	265
30	6	A		2500	300	10	5	>99	21	4.02	273
31	6	A	15	2500	300	13	7	>99	122, 2	2.03, 1.57	267
32	8	A		2500	1	100	≥15623	>99	36	1.32	271

[a]Conditions: 21 μmol of Sc, 21 μmol of activator, if [monomer]/[cat] < 2500, Tol/monomer = 5/1 (v/v) (other case is 30 mL of toluene), at room temperature. [b]act. = activator: A, [Ph$_3$C][B(C$_6$F$_5$)$_4$]; B, [PhMe$_2$NH][B(C$_6$F$_5$)$_4$]; C, B(C$_6$F$_5$)$_3$. [c]In units of (kg of polymer)/((mol of Sc) h). [d]Determined by ^{1}H and ^{13}C NMR. [e]Determined by high-temperature GPC in 1,2,4-trichlorobenzene at 140 °C. [f]Measured by DSC.

−0.47 (d, 2H, J = 11.2 Hz), −0.28 ppm (d, 2H, J = 10.8 Hz)). The methylene groups of the two CH$_2$SiMe$_3$ units in **5** appeared as a singlet at −1.14 ppm, while those in **6** showed two doublets at −1.25 and −1.13 ppm with geminal H−H coupling constants of 11.2 and 10.8 Hz. These results suggest that the free rotation of the CH$_2$SiMe$_3$ groups in **1**, **2**, and **5** might be possible, whereas the CH$_2$SiMe$_3$ groups in **3**, **4**, and **6** are fixed to some extent on the NMR time scale probably because of the greater steric hindrance of the fluorenyl ligands in **3**, **4**, and **6**.
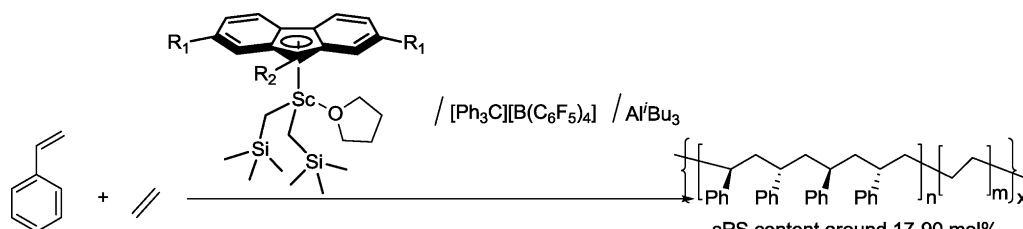
Syndiotactic Polymerization of Styrene. To gain fundamental information on the Al^{i}Bu$_3$ influence on the (co)polymerization activity and selectivity, the homopolymerization of styrene was first examined by use of the complexes Flu′Sc(CH$_2$SiMe$_3$)$_2$(THF)$_n$ (**1**−**6**) as catalyst precursors. [Ph$_3$C][B(C$_6$F$_5$)$_4$] (**A**), [PhMe$_2$NH][B(C$_6$F$_5$)$_4$] (**B**), and B-

(C$_6$F$_5$)$_3$ (**C**) were used as activators to abstract one alkyl group from the catalyst precursors. Representative results are summarized in Table 2.

By comparison, the complex **3**/**A** system showed lower activity (3.1 × 10^6 (g of polymer)/((mol of Sc) h)) than the known [(C$_5$Me$_4$SiMe$_3$)Sc(CH$_2$SiMe$_3$)(THF)][B(C$_6$F$_5$)$_4$] species generated by the (C$_5$Me$_4$SiMe$_3$)Sc(CH$_2$SiMe$_3$)$_2$(THF) (**8**)/[Ph$_3$C][B(C$_6$F$_5$)$_4$] catalytic system (1.6 × 10^7 (g of polymer)/((mol of Sc) h)) at a [monomer]/[catalyst] molar ratio of 2500, consistent with the fact that the cationic half-sandwich fluorenyl scandium complex has greater steric hindrance around the metal center than the cyclopentadienyl analogue (Table 2, entries 8 and 32). Surprisingly, the presence of a small amount of Al^{i}Bu$_3$ dramatically changed the catalytic performance of the complex **3**/**A** catalytic system in the styrene polymerization. Without

Table 3. Syndiospecific Copolymerization of Styrene and Ethylene by Fluo'Sc(CH$_2$SiMe$_3$)$_2$(THF)$_n$/[Ph$_3$C][B(C$_6$F$_5$)$_4$]/Al^{i}Bu$_3$ Catalytic Systems[a]

sPS content around 17–90 mol%

entry	cat.	[Al]/[Sc]	styrene (mmol)	yield (g)	act.[b]	PS cont[c] (mol %)	M_n[d] (×10^3)	M_w/M_n[d]	T_m[e] (°C)
1	4		0	trace					
2	4	15	0	0.3	429		3	3.57	124
3	4		31	0.02	27		10	1.13	273
4	2	15	31	3.3	4714	70	44	1.60	254
5	3	15	10	1.0	1429	24	18	3.05	122
6	3	15	21	2.5	3571	40	45	1.36	218
7	3	15	31	3.7	5286	59	69	1.46	262, 269
8	3	15	41	6.1	8714	73	71	1.19	258, 271
9	3	15	51	6.5	9286	80	94	1.83	262, 272
10	4	15	10	1.1	1571	17	3	1.57	126
11	4	15	21	2.9	4142	38	14	1.49	253, 263
12	4	15	31	4.3	6142	58	32	1.50	254, 267
13	4	15	41	5.5	7857	70	16	1.56	256, 267
14	4	15	51	6.7	9571	78	38	1.79	261, 270

[a]Conditions: 21 μmol of Sc, 21 μmol of activator, 1 atm of ethylene, 25 mL of toluene, 25 °C, 2 min. [b]In units of (kg of copolymer)/((mol of Sc) h atm). [c]Determined by ^{1}H NMR. [d]Determined by high temperature GPC in 1,2,4-trichlorobenzene at 140 °C. [e]Measured by DSC.

Al^{i}Bu$_3$, the complex **3**/A system only converted 88% styrene to polystyrene in 1 min when the [monomer]/[catalyst] molar ratio was 500 (Table 2, entry 7). If 2 equiv of Al^{i}Bu$_3$ was added, a slightly higher yield (about 90%) was obtained under the same conditions (Table 2, entry 9). In the presence of 10 or 15 equiv of Al^{i}Bu$_3$, however, 500 equiv of styrene could be completely transferred to the polystyrene in less than 1 min with an activity of up to 3.1 × 10^6 (g of polymer)/((mol of Sc) h), equal to that of the [(C$_5$Me$_4$SiMe$_3$)Sc(CH$_2$SiMe$_3$)(THF)][B(C$_6$F$_5$)$_4$] species under the same conditions (Table 2, entries 10 and 11). Remarkably, in comparison with the [(C$_5$Me$_4$SiMe$_3$)Sc-(CH$_2$SiMe$_3$)(THF)][B(C$_6$F$_5$)$_4$] species, which could not completely convert more than 2500 equiv of styrene in 1 min, the complex **3**/A/Al^{i}Bu$_3$ (15 equiv) system exhibited much higher activities and could completely convert 5500 equiv of styrene only in 1 min with activities up to 3.4 × 10^7 (g of polymer)/((mol of Sc) h) (Table 2, entries 12–19). On further increase of the [monomer]/[catalyst] molar ratio to 6000, however, only an 87% yield was obtained (Table 2, entry 20). Similar to the case for the trityl borate activator **A**, the anilinium borate activator **B** exhibited the same influence on the polymerization activity, while the neutral borane compound **C** showed a lower activity (Table 3, entries 21 and 22).

A significant influence of the fluorenyl ligand on the polymerization activity was also observed. Among the complexes **1**–**4** containing the THF molecule, **1**, bearing the simplest fluorenyl ligand (C$_{13}$H$_9$), showed the lowest activity, converting 2500 equiv of styrene into polystyrene within 60 min in the presence of 1 equiv of activator **A** and 15 equiv of Al^{i}Bu$_3$ at room temperature (Table 2, entry 1). With increasing electron density of the fluorenyl ligand in **2** (2,7-^{t}Bu$_2$-C$_{13}$H$_7$), **3** (9-SiMe$_3$-C$_{13}$H$_8$), and **4** (2,7-^{t}Bu$_2$-9-SiMe$_3$-C$_{13}$H$_6$), the styrene polymerizations became fast and only 1 min was required for completion in most cases. In comparison, the activity of these catalytic systems

increased in the order **2** < **4** < **3** (Table 2, entries 4, 20, and 25). These results are consistent with the polymerization performance of the half-sandwich group 3 or 4 catalysts, in which pentamethylcyclopentadienyl–scandium or –titanium catalysts showed higher activities than the corresponding cyclopentadienyl–scandium or –titanium analogues. However, complexes **5** and **6** bearing bidentate fluorenyl ligands had much worse activities (5–13 × 10^3 (g of polymer)/((mol of Sc) h)) than the THF-containing analogues **1**–**4** (Table 2, entries 28–31). Whether with or without the presence of Al^{i}Bu$_3$, only less than 25% yields were obtained in 300 min when the [monomer]/[catalyst] molar ratio was 2500.

The neutral complexes **1**–**6** alone were inactive under the same conditions, suggesting that the generation of a cationic metal alkyl species is essential for the present polymerization. The binary cationic fluorenyl species [Flu'Sc(CH$_2$SiMe$_3$)-(THF)][B(C$_6$F$_5$)$_4$] showed lower activity than the binary cationic cyclopentadienyl species [(C$_5$Me$_4$SiMe$_3$)Sc-(CH$_2$SiMe$_3$)(THF)][B(C$_6$F$_5$)$_4$] under the same conditions. In the presence of a small amount of Al^{i}Bu$_3$, however, the activity dramatically increased. These results demonstrate that the Al^{i}Bu$_3$ must have a considerable influence on the cationic scandium species, which completely changes the catalytic performance of the cationic species.

Notably, the microstructures of all the crude polystyrenes obtained by the complexes **1**–**6**/borate/Al^{i}Bu$_3$ systems were highly syndiotactic, with the pentad configuration rrrr >99% as determined by ^{13}C NMR (see the Supporting Information). Solvent fractionation demonstrated that neither atactic nor isotactic polystyrene was observed. The high syndiotacticity of the resulting polystyrenes was also confirmed by the high T_m values around 270 °C, a typical melting point for sPS.[9a] GPC profiles showed that the resulting sPSs obtained by the THF-containing complex **1**–**4**/activator/Al^{i}Bu$_3$ catalytic systems

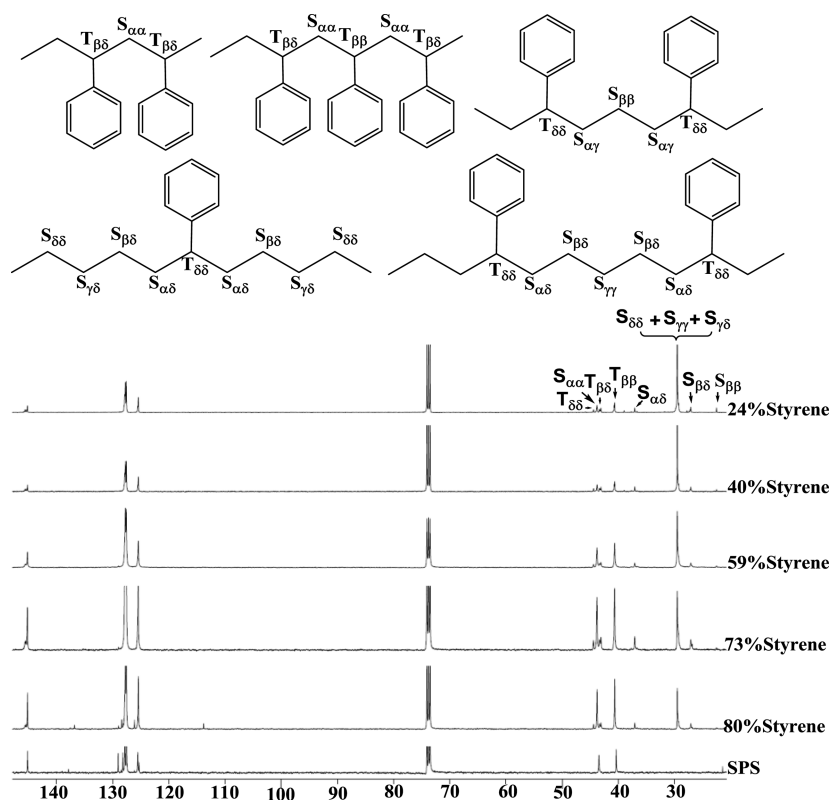**Figure 2.** ^{13}C NMR spectra of some representative copolymers obtained in Table 3.

possessed high molecular weights (M_n = 60000−780000 g/mol) with unimodal molecular weight distributions (M_w/M_n = 1.31−5.93), indicating the presence of a single-site active species during the styrene polymerization. In contrast, bimodal molecular weight distributions were obtained when the bidentate fluorenyl complexes **5** and **6**/A/Al^{i}Bu$_3$ catalytic systems were used as catalysts, implying the formation of more than one active species during the polymerization process.

Copolymerization of Styrene with Ethylene. The copolymerizations of styrene with ethylene had been carried out by feeding varying amounts of styrene under an atmosphere of ethylene (1 atm) in toluene at 25 °C in the presence of the half-sandwich scandium dialkyl complexes **2**−**4**, an activator, and 15 equiv of Al^{i}Bu$_3$, affording styrene−ethylene random copolymers containing syndiotactic styrene−styrene sequences. Representative results are shown in Table 3.

In the absence of styrene, the binary **4**/**A** catalytic system afforded only a trace amount of polyethylene at atmospheric pressure (Table 3, entry 1). In contrast, the ternary **4**/**A**/Al^{i}Bu$_3$ catalytic system showed moderate activity (4.3 × 10^5 (g of polyethylene)/((mol of Sc) h atm)) under the same conditions (Table 3, entry 2). In the copolymerization of styrene and ethylene, the ternary **4**/**A**/Al^{i}Bu$_3$ catalytic system exhibited 226 times higher activity (6.1 × 10^6 (g of copolymer)/((mol of Sc) h atm)) than the binary **4**/**A** catalytic system (2.7 × 10^4 (g of copolymer)/((mol of Sc) h atm)), affording the random copolymer with a styrene content of about 58 mol % (Table 3, entries 3 and 12). These results also testify to the different performances of the binary and ternary cationic half-sandwich scandium species in the copolymerization process.

The electron density and the steric environment around the scandium metal center of these fluorenyl scandium complexes induced by using different substituents on the fluorenyl ligand

not only determined the activity and syndiotactic selectivity in the copolymerization of styrene and ethylene but also governed the ethylene incorporation and distribution in the syndiotactic styrene−styrene sequences during the styrene−ethylene copolymerization process. The 2,7-^{t}Bu$_2$-substituted complex **2**/A/Al^{i}Bu$_3$ catalytic system showed relatively low activity (4.7 × 10^6 (g of copolymer)/((mol of Sc) h atm)) when 31 mmol of styrene was used under an atmosphere of ethylene (1 atm), affording a copolymer with a styrene content of about 70 mol % (Table 3, entry 4). For complex **3** bearing the trimethylsilyl (SiMe$_3$) group at 9-position on the fluorenyl ligand, with a gradual increase in the styrene feed from 10 to 51 mmol under 1 atm of ethylene, the copolymerization activities increased significantly from 1.4 × 10^6 to 9.3 × 10^6 (g of copolymer)/((mol of Sc) h atm) and the styrene contents in the resulting random copolymers increased gradually from 24 to 80 mol % (Table 3, entries 5−9). Complex **4** has 2,7-^{t}Bu$_2$ and 9-SiMe$_3$ substituents on the fluorenyl ring, and the complex **4**/A/Al^{i}Bu$_3$ catalytic system exhibited slightly higher activities ((1.6−9.6) × 10^6 (g of copolymer)/((mol of Sc) h atm)) than the complex **3**/A/Al^{i}Bu$_3$ catalytic system under the same conditions (Table 3, entries 10−14). However, the copolymers obtained had a somewhat lower styrene insertion (17−78 mol %) in comparison with those obtained by complex **3**/A/Al^{i}Bu$_3$ catalytic system. These results suggest that an increase of styrene feed under 1 atm of ethylene could accelerate the copolymerization of these two monomers. In contrast, the side-arm-coordinated complex **5** and **6**/A/Al^{i}Bu$_3$ catalytic systems could not promote the copolymerization of styrene with ethylene under the same conditions.

The copolymers obtained above are white elastomers. They have good solubility in 1,1,2,2-Cl$_4$C$_2$H$_2$ and o-C$_6$H$_4$Cl$_2$. GPC curves reveal that these copolymers possess moderate molecular weights (M_n = 3000−94000 g/mol) and unimodal molecular
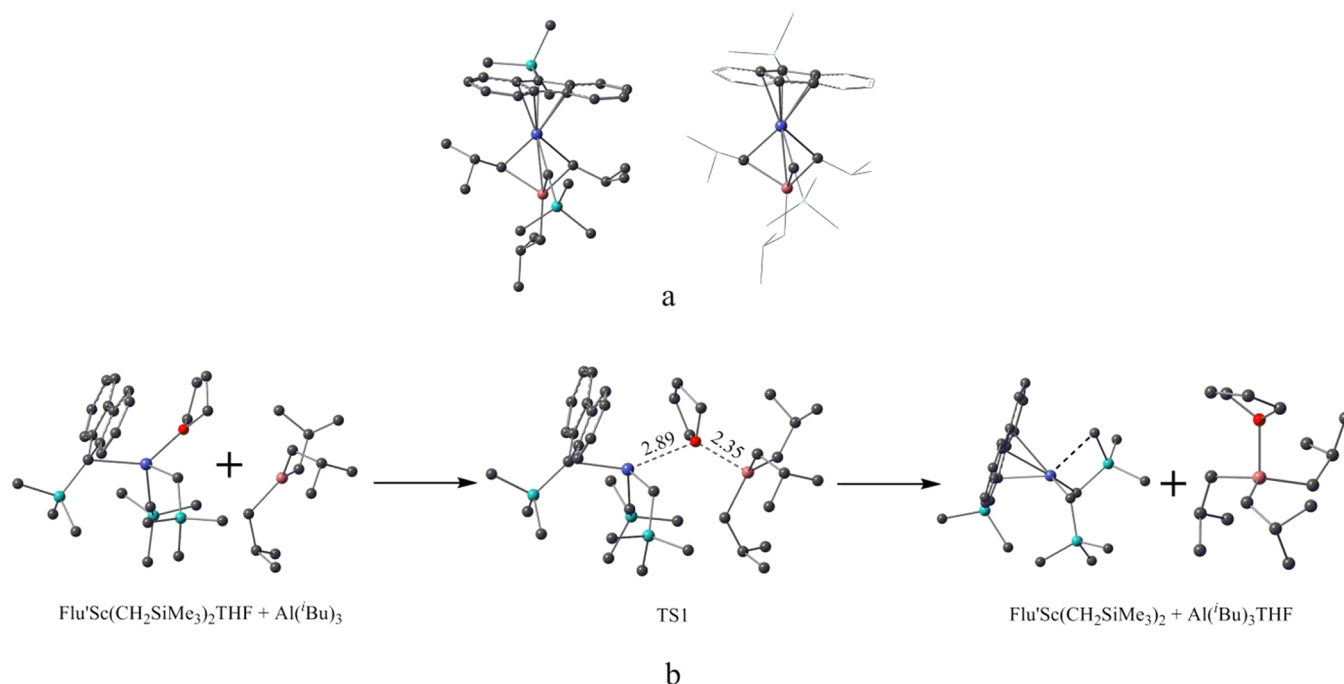
Figure 3. (a) Optimized structures of the bimetallic complex between Al^iBu_3 and $[(9\text{-}SiMe_3C_{13}H_8)Sc(CH_2SiMe_3)]^+$. (b) Optimized structures of the reactants, transition states, and products for the THF abstraction reaction $(9\text{-}SiMe_3C_{13}H_8)Sc(CH_2SiMe_3)_2(THF) + Al^iBu_3 \rightarrow (9\text{-}SiMe_3C_{13}H_8)Sc(CH_2SiMe_3)_2 + Al^iBu_3THF$. The $9\text{-}SiMe_3C_{13}H_8$ group is denoted as Flu′ for clarity.

weight distributions (1.13–3.12), indicative of the predominance of a homogeneous single-site catalytic species. Differential scanning calorimetry (DSC) demonstrated that the T_m values of these polymers vary in the range 253–272 °C, depending on the relative amounts of the syndiotactic polystyrene blocks in the copolymers. An endo peak corresponding to the melting point of polyethylene expected in the temperature range 120–130 °C was observed in the samples with elevated ethylene contents.

The ^{13}C NMR spectra of some typical copolymers are shown in Figure 2. Consistent with the selectivity observed in the homopolymerization of styrene, the styrene units in all the copolymers produced by the $2–4/A/Al^iBu_3$ catalytic systems adopted predominantly the syndiotactic microstructures (up to 90%), as evidenced by the peaks in ^{13}C NMR spectra at 145.7 (ipso-C), 45.0 ($S\alpha\alpha$), and 41.6 ppm ($T\beta\beta$) (Table 3 entries 4–20). The ethylene-rich copolymers (styrene content 24 mol % for **3** and 17 mol % for **4**) possessed almost random microstructures consisted of syndiotactic styrene–styrene sequences (blocks) connected by repeated ethylene units, as evidenced by the peaks at 27.1–27.8 (SEES, $S\beta\delta + S\beta\gamma$), 29.5 (SEES, EEE, EESEE, $S\delta\delta + S\gamma\delta + S\gamma\gamma$), 36.7–38.9 (SSS, ESSE, $S\alpha\delta$), 40.7 (SSS, $T\beta\beta$), 43.1–43.4 (ESSE, SSS, $T\beta\delta + S\alpha\alpha$), 44.4 (SEES, EESEE, $T\delta\delta + T\gamma\delta + T\gamma\gamma$), and 145.7 ppm (SSS, ipso-C) (Table 3, entries 5 and 10).[9a] In the styrene-rich copolymers (styrene content 70–94 mol %; Table 3, entries 8, 9, 13, 14, and 17–20), the signals of the PE units and random S–E units decreased, while those of sPS blocks largely increased (Figure 2). Signals for tail-to-tail or head-to-head styrene sequences were not observed (34–35 ppm, $S\alpha\beta$). These results are also consistent with what was observed from the binary **8**/A catalytic system.

Polymerization Mechanism. The experimental results mentioned above demonstrate that Al^iBu_3 really does have a dramatic effect on the catalytic performance of the binary cationic half-sandwich fluorenyl or cyclopentadienyl scandium alkyl species bearing THF as Lewis base in the syndiotactic

styrene polymerization and copolymerization with ethylene. During our (co)polymerization period, we found that the direct interaction of $Flu'Sc(CH_2SiMe_3)_2(THF)$ with Al^iBu_3 rapidly occurred in the presence of styrene, as testified by the darkening of the pale yellow of the catalyst precursor. A preliminary ^1H NMR spectrum of the combination of **3** and Al^iBu_3 showed that THF resonances shifted from δ 3.18 in **3** to δ 3.35, implying that THF molecule might be abstracted from the catalytic precursor to form Al^iBu_3THF.[13] To reveal the underlying mechanism at the molecular level, we performed quantum chemistry calculations on this catalytic reaction system. We attempted to make clear three questions: (1) what is the function of Al^iBu_3?; (2) how does Al^iBu_3 accelerate the catalytic reaction?; (3) what is the reason for the highly syndiospecific selectivity of the styrene polymerization? Figures 3–6 depict the calculated reaction paths that answer the above questions, respectively. For convenience to compare the energies of all the reactions, the standard Gibbs free energy at 298 K of all the reactants, intermediates, and transition states are shown in Figure 7. Later on, we refer to energy as the standard Gibbs free energy at 298 K for conciseness.

As mentioned above, Al^iBu_3 can react with a catalyst precursor to form a bimetallic complex. On the other hand, Al^iBu_3 may remove a THF molecule from the catalyst precursor and generate a new coordinatively unsaturated cationic species. In view of this, we performed calculations on two aspects of whether the Al^iBu_3 could form an active bimetallic complex or just remove a THF from the catalyst precursor.

After making a number of attempts, we could not find the bimetallic complexes between Al^iBu_3 and $(9\text{-}SiMe_3C_{13}H_8)Sc(CH_2SiMe_3)_2(THF)$ or $[(9\text{-}SiMe_3C_{13}H_8)Sc(CH_2SiMe_3)(THF)]^+$. However, we did find a bimetallic complex between Al^iBu_3 and $[(9\text{-}SiMe_3C_{13}H_8)Sc(CH_2SiMe_3)]^+$, as shown in Figure 3a. From this structure, we can see that there are three bridging CH_2 groups (two CH_2 come from two ^iBu and one CH_2 comes from CH_2SiMe_3) connecting the two metals Sc and Al.
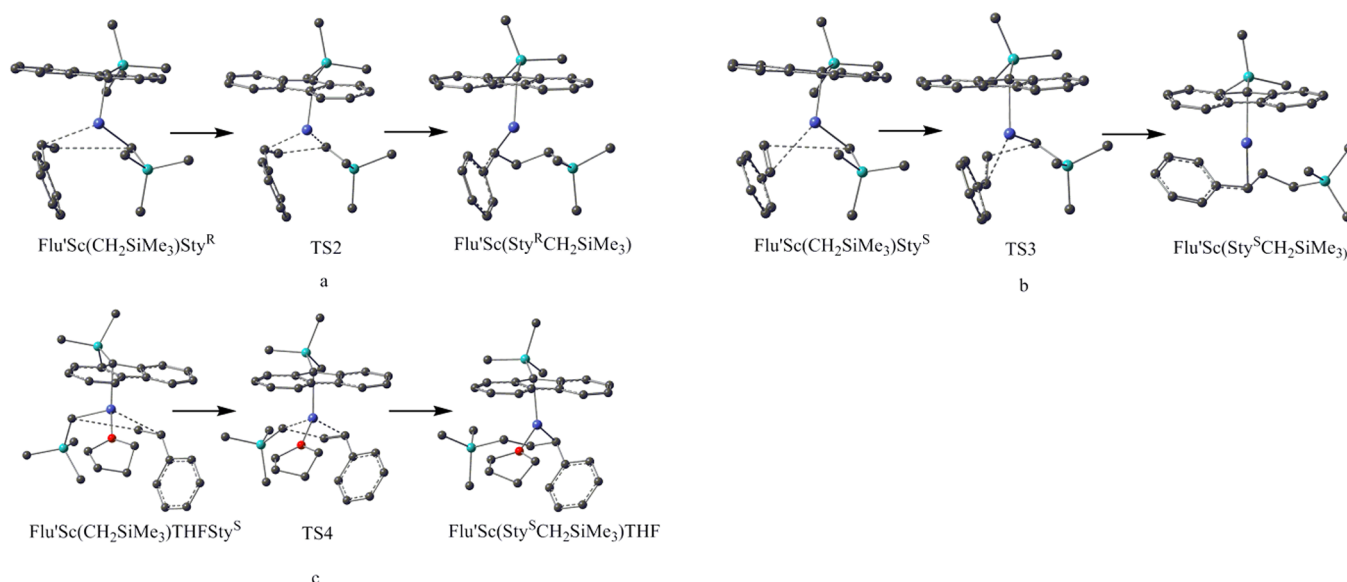
Figure 4. Optimized structures of the reactants, transition states, and products for the first styrene insertion reaction at the catalyst: (a) the *R* configuration insertion of styrene at $[(9\text{-SiMe}_3\text{C}_{13}\text{H}_8)\text{Sc}(\text{CH}_2\text{SiMe}_3)]^+$; (b) the *S* configuration coordination insertion of styrene at $[(9\text{-SiMe}_3\text{C}_{13}\text{H}_8)\text{Sc}(\text{CH}_2\text{SiMe}_3)]^+$; (c) the *S* configuration insertion of styrene at $[(9\text{-SiMe}_3\text{C}_{13}\text{H}_8)\text{Sc}(\text{CH}_2\text{SiMe}_3)(\text{THF})]^+$. The $9\text{-SiMe}_3\text{C}_{13}\text{H}_8$ group is denoted as Flu' for clarity.

Thus, the scanium center in this complex has achieved coordinative saturation. As a result, it is difficult to coordinate with another styrene molecule and initiation of polyolefin chain growth requires dissociation of the bound trialkylaluminum. In fact, we indeed could not locate a substantial coordinate complex between it and a styrene molecule during our calculations. Therefore, the presence of excess trialkylaluminum may inhibit or lower the catalytic efficiency and this bimetallic complex might not be catalytically active in such ternary systems.

On the other hand, we also calculated the THF transfer reaction mechanism $\text{Flu'Sc}(\text{CH}_2\text{SiMe}_3)_2(\text{THF}) + \text{Al}^i\text{Bu}_3 \rightarrow \text{Flu'Sc}(\text{CH}_2\text{SiMe}_3)_2 + \text{Al}^i\text{Bu}_3\text{THF}$. $(9\text{-SiMe}_3\text{C}_{13}\text{H}_8)\text{Sc}(\text{CH}_2\text{SiMe}_3)_2(\text{THF})$ (**3**) was chosen for DFT calculations. The calculated structures of the reactants, the transition state and the products are shown in Figure 3b. The corresponding energies of this reaction are given in Figure 7 (the dotted line in Figure 7).

From the structures in Figure 3b we can see that the THF transfer process is an elementary reaction. The distances between the oxygen atom of THF and the Sc and Al atoms are 2.89 and 2.35 Å, respectively, at the transition state. What should be mentioned is that the two (trimethylsilyl)methyl groups in **3** rearrange around the scandium center after the THF transfers to Al^iBu_3. An agostic bond shown as a dashed line in Figure 3b, which does not exist in the structure of **3**, is formed between the scandium center and a hydrogen atom in one methyl group of a (trimethylsilyl)methyl group. The agostic bond will enhance the bonding energy between the scandium center and the (trimethylsilyl)methyl group. The energy barrier height of the THF transfer reaction in Figure 7 is 22.4 kcal/mol, which enables the reaction to proceed at room temperature. Most importantly, the energy of the products $(9\text{-SiMe}_3\text{C}_{13}\text{H}_8)\text{Sc}(\text{CH}_2\text{SiMe}_3)_2 + \text{Al}^i\text{Bu}_3\text{THF}$ is only 0.1 kcal/mol higher than that of the reactants $(9\text{-SiMe}_3\text{C}_{13}\text{H}_8)\text{Sc}(\text{CH}_2\text{SiMe}_3)_2(\text{THF}) + \text{Al}^i\text{Bu}_3$. We can easily calculate the ratio of $(9\text{-SiMe}_3\text{C}_{13}\text{H}_8)\text{Sc}(\text{CH}_2\text{SiMe}_3)_2$ to $(9\text{-SiMe}_3\text{C}_{13}\text{H}_8)\text{Sc}(\text{CH}_2\text{SiMe}_3)_2(\text{THF})$ to be about 0.85:1 at thermal equilibrium by statistical thermodynamics theory. Namely, almost half of the $(9\text{-SiMe}_3\text{C}_{13}\text{H}_8)\text{Sc}(\text{CH}_2\text{SiMe}_3)_2(\text{THF})$ will transfer to $(9\text{-SiMe}_3\text{C}_{13}\text{H}_8)\text{Sc}$-

$(\text{CH}_2\text{SiMe}_3)_2$ with the presence of Al^iBu_3. Obviously, the latter has of course less steric effect than the former. In view of the fact that the product $(9\text{-SiMe}_3\text{C}_{13}\text{H}_8)\text{Sc}(\text{CH}_2\text{SiMe}_3)_2$ will be more easily activated by the coordination of a styrene molecule, the thermal equilibrium will shift to the formation of $(9\text{-SiMe}_3\text{C}_{13}\text{H}_8)\text{Sc}(\text{CH}_2\text{SiMe}_3)_2$. Thus, the main function of Al^iBu_3 is to remove a THF molecule from **3**, which transforms the $(9\text{-SiMe}_3\text{C}_{13}\text{H}_8)\text{Sc}(\text{CH}_2\text{SiMe}_3)_2(\text{THF})$ into $(9\text{-SiMe}_3\text{C}_{13}\text{H}_8)\text{Sc}(\text{CH}_2\text{SiMe}_3)_2$ as a new catalyst precursor. In the presence of 1 equiv of an activator such as $[\text{Ph}_3\text{C}][\text{B}(\text{C}_6\text{F}_5)_4]$, the (trimethylsilyl)methyl group that does not have an agostic bond with the scandium center will be abstracted away from the metal center and the new, THF-free cationic half-sandwich scandium alkyl species $[\text{Flu'Sc}(\text{CH}_2\text{SiMe}_3)][\text{B}(\text{C}_6\text{F}_5)_4]$ is generated.

To compare the catalytic activity of the ternary cationic active species $[(9\text{-SiMe}_3\text{C}_{13}\text{H}_8)\text{Sc}(\text{CH}_2\text{SiMe}_3)][\text{B}(\text{C}_6\text{F}_5)_4]$ to that of the binary $[(9\text{-SiMe}_3\text{C}_{13}\text{H}_8)\text{Sc}(\text{CH}_2\text{SiMe}_3)(\text{THF})][\text{B}(\text{C}_6\text{F}_5)_4]$ species in the styrene polymerization, we calculated the coordination and insertion reaction of styrene monomer to the scandium metal center during the initiation process. The optimized structures of these reaction paths are shown in Figure 4 (anion $[\text{B}(\text{C}_6\text{F}_5)_4]^-$ is omitted for clarity). The corresponding energies are given in Figure 7. It is found that no barrier is needed for the first styrene coordination to the scandium center. There are two orientations for a styrene to coordinate with the catalyst, as shown by the reactants in Figure 4a and 4b. Both coordination complexes can be characterized by the chiral carbon atoms in the growing polymer, i.e., the carbon atom of the ethylene that connects the benzene ring, which has been adopted by Hou and Luo to characterize the configuration of similar complexes.[14] According to the chirality of the carbon atom, Figure 4a,b exhibit *R* and *S* configurations of the styrene coordination and insertion reactions with the ternary cationic species $[(9\text{-SiMe}_3\text{C}_{13}\text{H}_8)\text{Sc}(\text{CH}_2\text{SiMe}_3)]^+$, respectively. Figure 4c shows the *S* configuration of the styrene coordination and insertion at the binary cationic species $[(9\text{-SiMe}_3\text{C}_{13}\text{H}_8)\text{Sc}(\text{CH}_2\text{SiMe}_3)(\text{THF})]^+$. The *R* configuration of the styrene coordination and insertion at $[(9\text{-}$
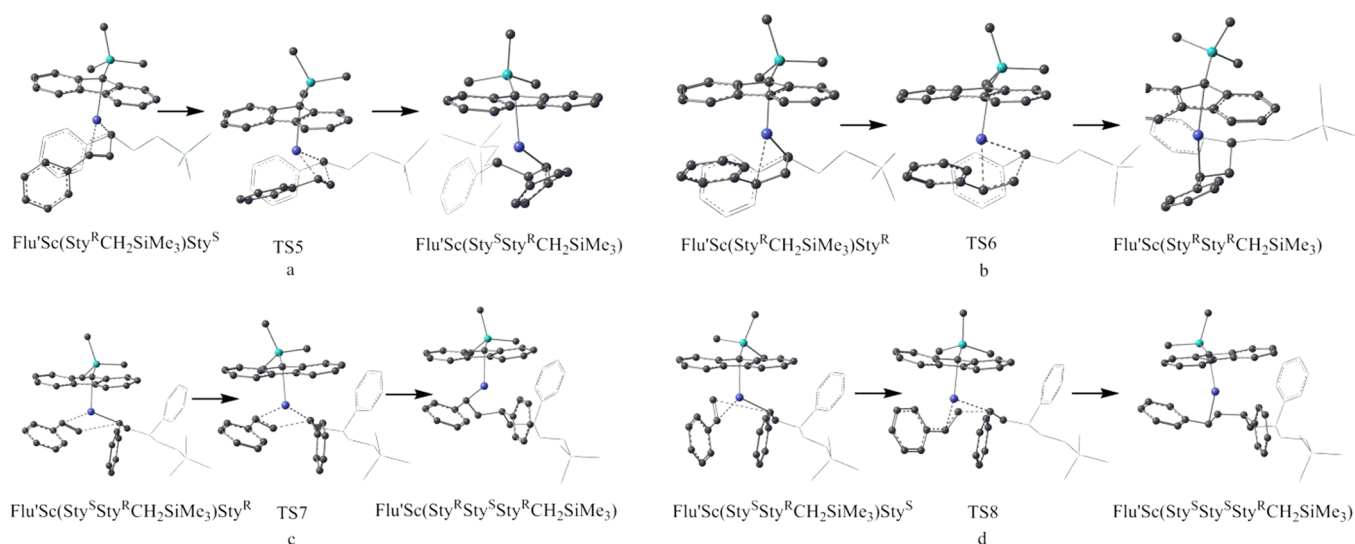
Figure 5. Optimized structures of the reactants, transition states, and products for the second and third styrene insertion reactions: (a) the *S* configuration insertion of the second styrene, producing the *R,S* configuration; (b) the *R* configuration insertion of the second styrene, producing the *R,R* configuration; (c) the *R* configuration insertion of the third styrene, producing the *R,S,R* configuration; (d) the *S* configuration insertion of the third styrene, producing the *R,S,S* configuration. The 9-SiMe$_3$C$_{13}$H$_8$ group is denoted as Flu′ for clarity.

SiMe$_3$C$_{13}$H$_8$)Sc(CH$_2$SiMe$_3$)(THF)]$^+$ is not given here due to its high reaction barrier and was not used for comparison with other reactions. Among these three coordination complexes in Figure 4, the *R* configuration complex [(9-SiMe$_3$C$_{13}$H$_8$)Sc(CH$_2$SiMe$_3$)-Sty^R]$^+$ (denoted as a′-Sty^R in Figure 7) has a binding energy of −8.8 kcal/mol, whereas the *S* configuration complex [[(9-SiMe$_3$C$_{13}$H$_8$)Sc(CH$_2$SiMe$_3$)Sty^S]$^+$ (denoted as a′-Sty^S in Figure 7) has a binding energy of −6.0 kcal/mol. In contrast, the *S* configuration complex [(9-SiMe$_3$C$_{13}$H$_8$)Sc(CH$_2$SiMe$_3$)(THF)-Sty^S]$^+$ (denoted as a′THF-Sty^S in Figure 7) has a binding energy of −7.4 kcal/mol. The difference in binding energy mainly originates from the steric effects of styrene with the surrounding chemical groups. During the insertion process, the barrier heights of the three reactions are found to differ greatly. In particular, the barrier height ca. 8.5 kcal/mol for the *R* configuration insertion of a′-Sty^R is much lower than that (ca. 22.1 kcal/mol) of the *S* configuration insertion of a′-Sty^S, indicating that the *R* configuration will dominate the first styrene coordination and insertion reaction to the ternary cationic species [[(9-SiMe$_3$C$_{13}$H$_8$)Sc(CH$_2$SiMe$_3$)][B(C$_6$F$_5$)$_4$]. By comparison, the barrier height for the *S* configuration insertion of a′THF-Sty^S is 10.2 kcal/mol, which is ca. 1.7 kcal/mol higher than that for a′-Sty^R due to the greater steric repulsion from THF. Moreover, the steric repulsion from THF will become more obvious with the increasing polymer chain. As a result, the styrene polymerization catalyzed by the ternary cationic species [[(9-SiMe$_3$C$_{13}$H$_8$)Sc-(CH$_2$SiMe$_3$)][B(C$_6$F$_5$)$_4$] is expected to be much faster than that by the binary cationic species [[(9-SiMe$_3$C$_{13}$H$_8$)Sc(CH$_2$SiMe$_3$)-(THF)][B(C$_6$F$_5$)$_4$]. This result perfectly answers the question why Al^{i}Bu$_3$ accelerates the catalytic reaction.

On the basis of the calculations above, we knew that the coordination and insertion reaction of the first styrene to the cation [(9-SiMe$_3$C$_{13}$H$_8$)Sc(CH$_2$SiMe$_3$)]$^+$ adopts the *R* configuration. We were then interested to calculate which configuration should be taken up in the coordination and insertion reaction of the second styrene at [(9-SiMe$_3$C$_{13}$H$_8$)Sc(Sty^{R}CH$_2$SiMe$_3$)]$^+$ (denoted as a′-Sty$_1^R$ in Figure 7). Similarly, the second styrene coordinates to the scandium center in two orientations, i.e., the *R* configuration and the *S* configuration. Parts a and b of Figure 5

give the reaction paths of the *S* and the *R* configuration coordination and insertion of the second styrene, respectively. The corresponding energies are shown in Figure 7. From the structure of a′-Sty$_1^R$, we can see that there is a channel between the fluorenyl ring and the benzene ring of the first styrene, which is the coordination site of the second styrene to the scandium center. Thus, the steric effect of this channel is very important for the *R* and *S* configuration coordination and insertion of the second styrene. Figure 7 shows that the energy of the *S* configuration coordination complex [(9-SiMe$_3$C$_{13}$H$_8$)Sc-(Sty^{R}CH$_2$SiMe$_3$)Sty^S]$^+$ (denoted as a′-Sty$_1^R$-Sty^S in Figure 7) is about 1.4 kcal/mol lower than that of the *R* configuration coordination complex [(9-SiMe$_3$C$_{13}$H$_8$)Sc(Sty^{R}CH$_2$SiMe$_3$)-Sty^R]$^+$ (denoted as a′(Sty)$_1^R$-Sty^R in Figure 7). Moreover, the barrier height of the *S* configuration insertion ([[(9-SiMe$_3$C$_{13}$H$_8$)-Sc(Sty^{S}Sty^{R}CH$_2$SiMe$_3$)]$^+$, denoted as a′-(Sty)$_1^R$Sty^S in Figure 7, 4.2 kcal/mol) is much lower than that of the *R* configuration insertion (([[(9-SiMe$_3$C$_{13}$H$_8$)Sc(Sty^{R}Sty^{R}CH$_2$SiMe$_3$)]$^+$, denoted as a′-(Sty)$_1^R$Sty^R in Figure 7, 22.0 kcal/mol). Obviously, the *S* configuration insertion reaction will dominate the polymerization growth of the second styrene.

The calculated reaction paths for the *R* and *S* configuration coordination and insertion of the third styrene are shown in parts c and d of Figure 5, respectively. What should be pointed out is that we employed the QM/MM method in the calculation of the coordination and insertion of the third styrene due to the limitation of our computation resources. The QM/MM method is described in Computational Details. The channel in the structure of the second styrene insertion product a′-(Sty)$_1^R$Sty^S indicates that the third styrene will coordinate to the scandium center in the same direction as the first styrene does. The calculated energies, which are provided in the Supporting Information, indicate that the reaction barrier of the *R* configuration insertion (6.2 kcal/mol) is much lower than that of the *S* configuration insertion (25.3 kcal/mol). Therefore, the *R* configuration insertion reaction will dominate the polymerization growth of the third styrene.

Then, our question was this: which configuration would dominate for the coordination and insertion of the fourth and the
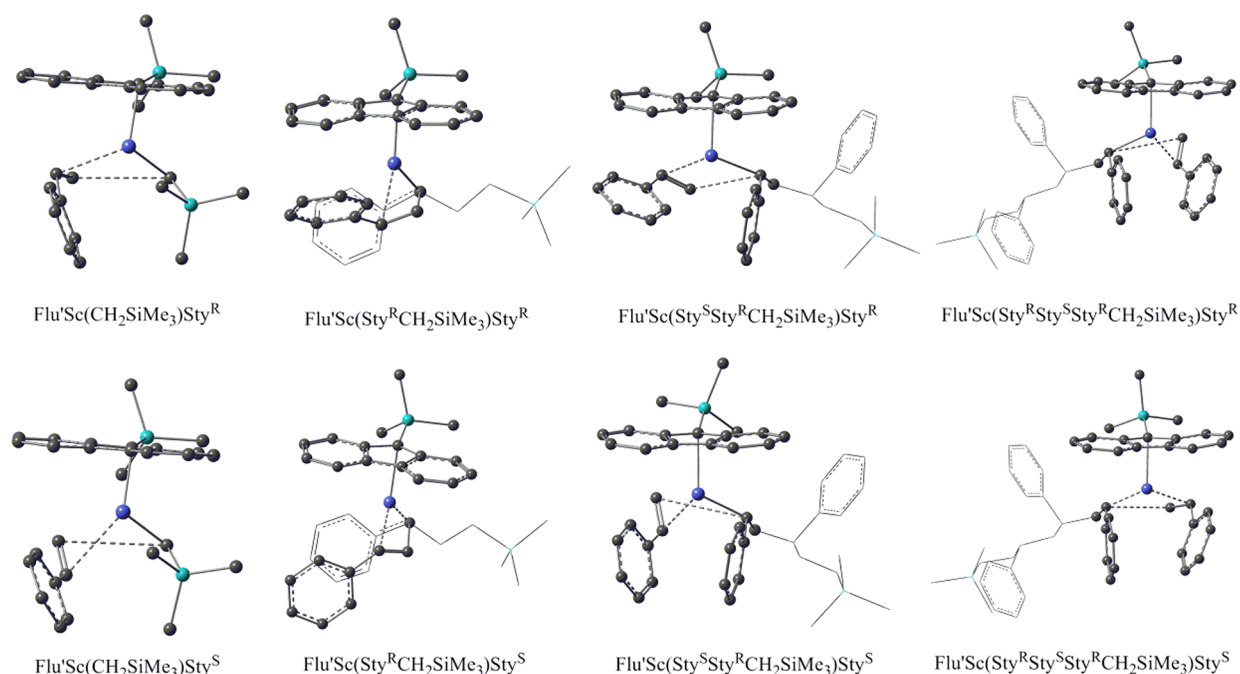
Figure 6. Structures of the *R* and *S* configurations for the coordination complexes of the catalyst with the first, second, third, and fourth styrenes. The *R*/ *S* configuration complexes of the first, second, third, and fourth styrene sare $[Flu'Sc(CH_2SiMe_3)Sty^R]^+/[Flu'Sc(CH_2SiMe_3)Sty^S]^+$, $[Flu'Sc-(Sty^RCH_2SiMe_3)Sty^R]^+/[Flu'Sc(Sty^RCH_2SiMe_3)Sty^S]^+$, $[Flu'Sc(Sty^SSty^RCH_2SiMe_3)Sty^R]^+/[Flu'Sc(Sty^SSty^RCH_2SiMe_3)Sty^S]^+$, and $[Flu'Sc-(Sty^RSty^SSty^RCH_2SiMe_3)Sty^R]^+/[Flu'Sc(Sty^RSty^SSty^RCH_2SiMe_3)Sty^S]^+$, respectively. The dashed lines mark the atoms that will form chemical bonds in the following insertion reaction. The $9\text{-}SiMe_3C_{13}H_8$ group is denoted as Flu' for clarity.
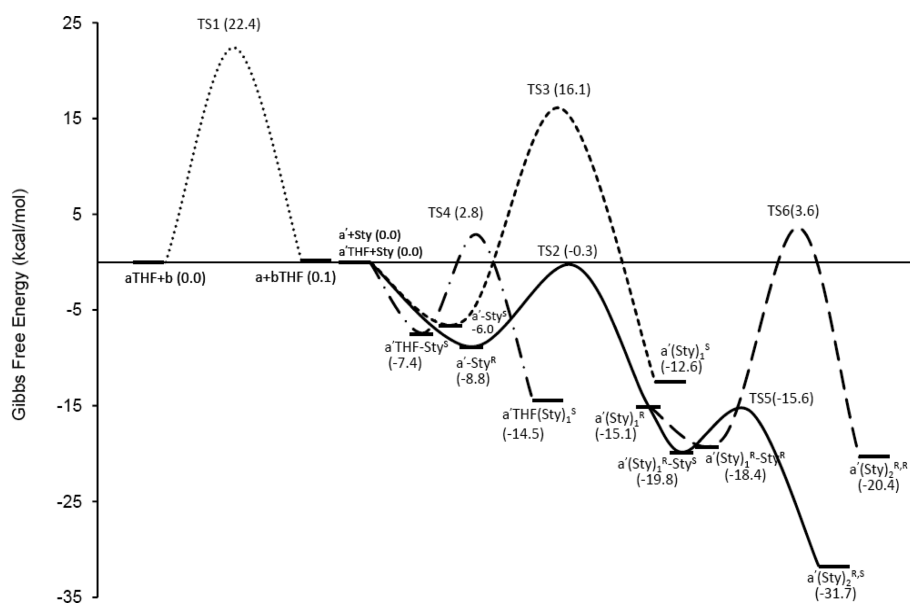
Figure 7. Gibbs free energy profiles of all the reaction paths. For the purpose of conciseness, we adopt some symbols in this figure to represent the compounds appearing in Figures 3−6 and in the text, where a = $(9\text{-}SiMe_3C_{13}H_8)Sc(CH_2SiMe_3)_2$, b = Al^iBu_3, a' = $(9\text{-}SiMe_3C_{13}H_8)Sc(CH_2SiMe_3)$, Sty = styrene, the superscripts *R* and *S* of Sty represent the *R* or *S* configuration, and the subscripts 1 and 2 represent the number of styrenes inserted. For conciseness and consistency, the zero points of the Gibbs free energy profiles are different for different reactions in order to keep the number of atoms unchanged for each reaction path; specifically, the zero point for the stepwise reaction path from a'+Sty to $a'(Sty)_2^{R,S}/a'(Sty)_2^{R,R}$ is set to the energy of a'+2Sty. The zero point for other elementary reaction paths is set to the total energy of the corresponding reactants.

following successive styrenes? In order to answer this question, we optimized further the structures of the coordination cation of the fourth styrene with the products of the third styrene insertion. Figure 6 depicts the coordination structures of the scandium center with the first, second, third, and fourth styrene adopting both the *R* and *S* configurationd. After carefully

analyzing the characteristics of these structures, we can directly observe that there is a certain relationship between the insertion quadrangle consisting of the double bond of styrene, the bond of scandium with the methene carbon of polymer, and the two forming bonds shown as dashed lines in Figure 6. On the basis of the fact that the first $(Flu'Sc(CH_2SiMe_3)Sty^R)$ and third styrene

coordinations and insertions (Flu′Sc(Sty^{S}Sty^{R}CH$_2$SiMe$_3$)Sty^R) adopt the R configuration and the second styrene coordination and insertion (Flu′Sc(Sty^{R}CH$_2$SiMe$_3$)Sty^S) takes up the S configuration, the dominant configurations are those in which the insertion quadrangle are almost on the same plane and the two opposite bonds are approximately parallel. This is probably because these configurations will bring about less structural change and thus induce less steric repulsion as the styrene insertion proceeds. Obviously, the insertion quadrangle in the S configuration of the fourth styrene coordination complex (Flu′Sc(Sty^{R}Sty^{S}Sty^{R}CH$_2$SiMe$_3$)Sty^S) is close to coplanar. As a result, the dominant S configuration of the fourth styrene will coordinate to the scandium cation in the same way as the second styrene. In view of the alternative coordination position of the styrene to the opposite side of the cationic scandium center, the propagation process of styrene at the cationic scandium−polymer chain will adopt the R−S−R−S··· insertion sequence. Such a sequence will finally result in syndiotactic polystyrene, as pointed out by Hou and Luo.[13] It is worth mentioning that the reaction barrier of the dominant configuration is always much lower than the other configuration at each coordination and insertion process, which is the origin of the highly syndiotactic selectivity. To our knowledge, DFT calculations on the Al^{i}Bu$_3$ effect in the ternary cationic half-sandwich scandium system and the mechanism of the syndiotactic styrene polymerization by such ternary catalytic system have not been reported previously.

■ CONCLUSION

In summary, the series of half-sandwich scandium dialkyl complexes **1**−**6**, bearing various substituted fluorenyl ligands and Lewis bases, have been synthesized and structurally characterized. The experimental results demonstrate that Al^{i}Bu$_3$ really does have a dramatic acceleration effect on the catalytic performance of the binary cationic half-sandwich fluorenyl scandium alkyl species bearing THF as a Lewis base in the syndiotactic styrene polymerization and copolymerization with ethylene. However, such a dramatic aluminum effect cannot be observed when the bidentate fluorenyl complexes **5** and **6** (Flu′Sc(CH$_2$SiMe$_3$)$_2$), having a nitrogen−heteroatom-coordinated side arm, are used as catalyst precursors. Moreover, the steric hindrance and the electron density around the scandium center of cationic active species also play a role in the catalytic activity and the comonomer incorporation and distribution in the copolymer chain. DFT calculations on the truly active species by using the representative catalyst show that the formation of the heterobinuclear Sc−isobutyl−Al complexes inhibited the styrene (co)polymerization. Instead, Al^{i}Bu$_3$ can capture the THF molecule from the half-sandwich fluorenyl scandium dialkyl complexes **1**−**4** at first. Then the new, THF-free cationic half-sandwich scandium active species [Flu′Sc(CH$_2$SiMe$_3$)][B-(C$_6$F$_5$)$_4$] with less steric hindrance around the metal center is generated in the presence of 1 equiv of an activator such as [Ph$_3$C][B(C$_6$F$_5$)$_4$]. DFT calculations on the initiation process demonstrate that the barrier height for the R configuration insertion of the first styrene into the ternary active species [Flu′Sc(CH$_2$SiMe$_3$)][B(C$_6$F$_5$)$_4$] is lower than that of the R or S configuration insertion of the first styrene into the binary active species [Flu′Sc(CH$_2$SiMe$_3$)(THF)][B(C$_6$F$_5$)$_4$]. This result perfectly answers the question why Al^{i}Bu$_3$ accelerates the catalytic reaction. The energy barriers of the propagation processes indicate that the consecutive insertion of styrenes at the cationic scandium−polymer chain adopt the R−S−R−S··· configurations, which finally results in the syndiotactic

polystyrene and syndiotactic styrene−styrene sequence in the styrene−ethylene copolymer. In contrast, the nitrogen−heteroatom-coordinated side arm of the bidentate fluorenyl complexes **5** and **6** cannot be abstracted away from the scandium cation by Al^{i}Bu$_3$ in most cases, which results in the absence of a dramatic aluminum effect and the presence of two active species in the styrene polymerization. Although olefin (co)-polymerizations by various ternary cationic catalytic systems have been studied extensively, such a full understanding on the dramatic Al^{i}Bu$_3$ effect and the activation mechanism based on DFT studies is, to our knowledge, limited. We believe that these DFT calculation results should shed new light on improving the catalytic performance of the conventional Ziegler−Natta catalysts and designing novel, excellent molecular catalysts for precise olefin polymerization. Further research into the systematic determination of the structure−activity relationship of this catalytic system in other olefin polymerizations is underway.

■ EXPERIMENTAL SECTION

Materials. All manipulations of air- and moisture-sensitive compounds were performed under a dry nitrogen atmosphere by use of standard Schlenk techniques or a nitrogen-filled Mbraun glovebox. Nitrogen and ethylene (Beijing AP Beifen Gases Industrial Co., Ltd.) were purified by being passed through a Dryclean column (4 A molecular sieves, Dalian Replete Science And Technology Co., Ltd.) and a Gasclean CC-XR column (Dalian Replete Science And Technology Co., Ltd.). Anhydrous toluene, THF, and hexane were purified by use of a SPS-800 solvent purification system (Mbraun) and dried over fresh Na chips in the glovebox. Styrene was purchased from TCI, dried over CaH$_2$, vacuum-transferred, and degassed by two freeze−pump−thaw cycles prior to polymerization experiments. ScCl$_3$ was purchased from Strem. C$_{13}$H$_{10}$ was purchased from Aldrich and used as received. Other fluorenyl ligands such as 2,7-^{t}Bu$_2$C$_{13}$H$_7$, 9-SiMe$_3$C$_{13}$H$_8$, 2,7-^{t}Bu$_2$-9-SiMe$_3$C$_{13}$H$_6$, 9-CH$_2$CH$_2$NMe$_2$C$_{13}$H$_8$, and 2,7-^{t}Bu$_2$-9-CH$_2$CH$_2$NMe$_2$C$_{13}$H$_6$ were synthesized according to the literature.[15] nBuLi (2.8 M solution in pentane), LiCH$_2$SiMe$_3$ (1.0 M solution in pentane), and Al^{i}Bu$_3$ (1.1 M solution in toluene) were purchased from Aldrich and used as received. [Ph$_3$C][B(C$_6$F$_5$)$_4$], [PhMe$_2$NH][B-(C$_6$F$_5$)$_4$], and B(C$_6$F$_5$)$_3$ were purchased from Tosoh Finechem Corp. and used without purification. The deuterated solvents benzene-d_6 (99.6 atom % D), CDCl$_3$-d (99.8 atom % D), and 1,1,2,2-tetrachloroethane-d_2 (99.6 atom % D) were obtained from Cambridge Isotope.

General Methods. Samples of rare-earth-metal complexes for NMR spectroscopic measurements were prepared in the glovebox using J. Young valve NMR tubes. The NMR (^{1}H, ^{13}C) spectra of catalyst precursors were recorded on an AVANCE 400 spectrometer at room temperature with C$_6$D$_6$ as a solvent. ^{1}H and ^{13}C NMR spectra of polystyrene and copolymer samples obtained by cationic half-sandwich scandium species were recorded on an AVANCE 400 spectrometer in 1,1,2,2-tetrachloroethane-d_2 at 60 °C. Elemental analyses were performed on an Elementar Vario MICRO CUBE instrument (Germany). The molecular weights and the molecular weight distributions of the polystyrene and copolymer samples were determined at 140 °C by high-temperature gel permeation chromatography (HT-GPC) on a PL220/HT apparatus (Tosoh Corp.). 1,3,5-Trichlorobenzene (TCB) was employed as the eluent at a flow rate of 1.0 mL/min. The calibration was made by the polystyrene standard EasiCal PS-1 (PL Ltd.). The DSC measurements were performed on a TA60 instrument (TA Co.) at a rate of 10 °C/min. Any thermal history difference in the polymers was eliminated by first heating the specimen to 300 °C, cooling to 40 °C, and then recording the second DSC scan.

Synthesis of (Flu)Sc(CH$_2$SiMe$_3$)$_2$(THF) (1). ScCl$_3$ (0.076 g, 0.50 mmol) was refluxed in 10 mL of THF at 100 °C for 12 h. The solution was cooled with stirring at room temperature to give a white suspension of ScCl$_3$(THF)$_3$. A THF solution (5 mL) of FluLi (0.086 g, 0.50 mmol), which was prepared by the reaction of fluorenyl (Flu) with n-BuLi (0.21 mL, 0.50 mmol), was added slowly, and the mixture was stirred at room temperature for 3.5 h. A THF solution (3 mL) of Me$_3$SiCH$_2$Li (0.094 g,

1.00 mmol) was then added slowly. After the mixture was stirred at room temperature for 30 min, the solvent was removed under vacuum. The residue was extracted with hexane. The hexane extract was concentrated under vacuum and kept at −30 °C to give **1** as pale yellow solids (0.18 g, 0.40 mmol, 80% yield). ^{1}H NMR (400 MHz, C$_6$D$_6$, 22 °C, δ/ppm): −0.11 (s, 4H, CH_2Si(CH$_3$)$_3$), 0.29 (s, 18H, CH$_2$Si(CH_3)$_3$), 1.31 (m, 4H, THF-β-CH_2), 3.68 (m, 4H, THF-α-CH_2), 4.04 (t, 1H, 9-CH-fluorenyl), 7.16−7.65 (m, 9H, fluorenyl). ^{13}C NMR (100 MHz, C$_6$D$_6$): 4.4, 25.4, 37.0, 67.4, 120.2, 124.5, 125.3, 127.0, 127.1, 127.4, 141.8, 142.2, 143.6, 147.4. Anal. Calcd for C$_{25}$H$_{39}$OScSi$_2$: C, 65.75; H, 8.61. Found: C, 65.28; H, 8.25.

Synthesis of (2,7-^{t}Bu$_2$Flu)Sc(CH$_2$SiMe$_3$)$_2$(THF) (2). ScCl$_3$ (0.076 g, 0.50 mmol) was refluxed in 10 mL of THF at 100 °C for 12 h. The solution was cooled with stirring at room temperature to give a white suspension of ScCl$_3$(THF)$_3$. A THF solution (5 mL) of 2,7-^{t}Bu$_2$FluLi (0.14 g, 0.50 mmol), which was prepared by the reaction of 2,7-^{t}Bu$_2$Flu with n-BuLi (0.21 mL, 0.50 mmol), was added slowly and stirred at room temperature for 3.5 h. A THF solution (3 mL) of Me$_3$SiCH$_2$Li (0.094 g, 1.00 mmol) was then added slowly. After the mixture was stirred at room temperature for 30 min, the solvent was removed under vacuum. The residue was extracted with hexane. The hexane extract was concentrated under vacuum and kept at −30 °C to give **2** as yellow solids (0.22 g, 0.38 mmol, 76% yield). ^{1}H NMR (400 MHz, C$_6$D$_6$, 22 °C, δ/ppm): −0.06 (s, 4H, CH_2Si(CH$_3$)$_3$), 0.29 (s, 18H, CH$_2$Si(CH_3)$_3$), 1.28 (m, 4H, THF-β-CH_2), 1.39 (s, 18H, C(CH_3)$_3$), 3.81 (m, 4H, THF-α-CH_2), 4.08 (t, 1H, 9-CH-fluorenyl), 7.16−7.68 (m, 7H, fluorenyl). ^{13}C NMR (100 MHz, C$_6$D$_6$): 4.0, 21.5, 31.4, 35.0, 46.0, 62.9, 95.9, 114.1, 116.2, 119.1, 122.8, 124.1, 131.6, 147.9. Anal. Calcd for C$_{33}$H$_{55}$OScSi$_2$: C, 69.67; H, 9.74. Found: C, 69.96; H, 9.96.

Synthesis of (9-SiMe$_3$Flu)Sc(CH$_2$SiMe$_3$)$_2$(THF) (3). ScCl$_3$ (0.076 g, 0.50 mmol) was refluxed in 10 mL of THF at 100 °C for 12 h. The solution was cooled with stirring at room temperature to give a white suspension of ScCl$_3$(THF)$_3$. A THF solution (5 mL) of 9-SiMe$_3$FluLi (0.12 g, 0.50 mmol), which was prepared by the reaction of 9-SiMe$_3$Flu with n-BuLi (0.21 mL, 0.50 mmol), was added slowly and stirred at room temperature for 3.5 h. A THF solution (3 mL) of Me$_3$SiCH$_2$Li (0.094 g, 1.00 mmol) was then added slowly. After the mixture was stirred at room temperature for 30 min, the solvent was removed under vacuum. The residue was extracted with hexane. The hexane extract was concentrated under vacuum and kept at −30 °C to give **3** as yellow crystals (0.20 g, 0.39 mmol, 77% yield). ^{1}H NMR (400 MHz, C$_6$D$_6$, 22 °C, δ/ppm): −0.41 (d, 2H, J = 11.2 Hz, CH_2Si(CH$_3$)$_3$), −0.25 (d, 2H, J = 11.6 Hz, CH_2Si(CH$_3$)$_3$), 0.13 (s, 18H, CH$_2$Si(CH_3)$_3$), 0.66 (s, 9H, Si(CH_3)$_3$), 1.04 (m, 4H, THF-β-CH_2), 3.18 (m, 4H, THF-α-CH_2), 7.02−8.04 (m, 8H, fluorenyl). ^{13}C NMR (100 MHz, C$_6$D$_6$): 2.1, 3.9, 24.6, 47.6, 71.4, 93.2, 120.4, 122.2, 124.8, 125.2, 125.7, 138.7. Anal. Calcd for C$_{28}$H$_{47}$OScSi$_3$: C, 63.59; H, 8.96. Found: C, 63.77; H, 9.27.

Synthesis of (2,7-^{t}Bu$_2$-9-SiMe$_3$Flu)Sc(CH$_2$SiMe$_3$)$_2$(THF) (4). ScCl$_3$ (0.076 g, 0.50 mmol) was refluxed in 10 mL of THF at 100 °C for 12 h. The solution was cooled with stirring at room temperature to give a white suspension of ScCl$_3$(THF)$_3$. A THF solution (5 mL) of 2,7-^{t}Bu$_2$-9-SiMe$_3$FluLi (0.18 g, 0.50 mmol), which was prepared by the reaction of 2,7-^{t}Bu$_2$-9-SiMe$_3$Flu with n-BuLi (0.21 mL, 0.50 mmol), was added slowly and stirred at room temperature for 3.5 h. A THF solution (3 mL) of Me$_3$SiCH$_2$Li (0.094 g, 1.00 mmol) was then added slowly. After the mixture was stirred at room temperature for 30 min, the solvent was removed under vacuum. The residue was extracted with hexane. The hexane extract was concentrated under vacuum and kept at −30 °C to give **4** as yellow crystals (0.21 g, 0.33 mmol, 65% yield). ^{1}H NMR (400 MHz, C$_6$D$_6$, 22 °C, δ/ppm): −0.47 (d, 2H, J = 11.2 Hz, CH_2Si(CH$_3$)$_3$), −0.28 (d, 2H, J = 10.8 Hz, CH_2Si(CH$_3$)$_3$), 0.13 (s, 18H, CH$_2$Si(CH_3)$_3$), 0.75 (s, 9H, Si(CH_3)$_3$), 1.37 (m, 4H, THF-β-CH_2), 1.43 (s, 18H, C(CH_3)$_3$), 3.53 (m, 4H, THF-α-CH_2), 7.21−8.12 (m, 6H, fluorenyl). ^{13}C NMR (100 MHz, C$_6$D$_6$): 2.1, 4.0, 24.7, 31.7, 35.2, 46.8, 71.3, 93.3, 119.6, 120.4, 121.8, 122.4, 139.5, 147.6. Anal. Calcd for C$_{36}$H$_{63}$OScSi$_3$: C, 67.44; H, 9.90. Found: C, 67.02; H, 9.35.

Synthesis of (9-CH$_2$CH$_2$NMe$_2$Flu)Sc(CH$_2$SiMe$_3$)$_2$ (5). ScCl$_3$ (0.076 g, 0.50 mmol) was refluxed in 10 mL of THF at 100 °C for 12 h. The solution was cooled with stirring at room temperature to give a white suspension of ScCl$_3$(THF)$_3$. A THF solution (5 mL) of 9-CH$_2$CH$_2$NMe$_2$FluLi (0.13 g, 0.50 mmol), which was prepared by the reaction of 9-CH$_2$CH$_2$NMe$_2$Flu with n-BuLi (0.21 mL, 0.50 mmol), was added slowly and stirred at room temperature for 3.5 h. A THF solution (3 mL) of Me$_3$SiCH$_2$Li (0.094 g, 1.00 mmol) was then added slowly. After the mixture was stirred at room temperature for 30 min, the solvent was removed under vacuum. The residue was extracted with hexane. The hexane extract was concentrated under vacuum and kept at −30 °C to give **5** as yellow crystals (0.18 g, 0.39 mmol, 77% yield). ^{1}H NMR (400 MHz, C$_6$D$_6$, 22 °C, δ/ppm): −1.14 (s, 4H, CH_2Si(CH$_3$)$_3$), 0.13 (s, 18H, CH$_2$Si(CH_3)$_3$), 1.88 (s, 6H, N(CH_3)$_2$), 2.38 (t, 2H, J = 6.2 Hz, CH$_2$CH_2N(CH$_3$)$_2$), 2.64 (t, 2H, J = 6.2 Hz, CH_2CH$_2$N(CH$_3$)$_2$), 7.15−8.20 (m, 8H, fluorenyl). ^{13}C NMR (400 MHz, C$_6$D$_6$): 3.9, 21.6, 31.5, 46.0, 62.9, 95.9, 118.5, 119.5, 119.9, 124.7, 125.9, 131.1. Anal. Calcd for C$_{25}$H$_{40}$NScSi$_2$: C, 65.89; H, 8.85; N, 3.07. Found: C, 65.48; H, 8.55; N, 3.49.

Synthesis of (2,7-^{t}Bu$_2$-9-CH$_2$CH$_2$NMe$_2$Flu)Sc(CH$_2$SiMe$_3$)$_2$ (6). ScCl$_3$ (0.076 g, 0.50 mmol) was refluxed in 10 mL of THF at 100 °C for 12 h. The solution was cooled with stirring at room temperature to give a white suspension of ScCl$_3$(THF)$_3$. A THF solution (5 mL) of 2,7-^{t}Bu$_2$-9-CH$_2$CH$_2$NMe$_2$Flu-Li (0.18 g, 0.50 mmol), which was prepared by the reaction of 2,7-^{t}Bu$_2$-CH$_2$CH$_2$NMe$_2$Flu with n-BuLi (0.21 mL, 0.50 mmol), was added slowly and stirred at room temperature for 3.5 h. A THF solution (3 mL) of Me$_3$SiCH$_2$Li (0.094 g, 1.00 mmol) was then added slowly. After the mixture was stirred at room temperature for 30 min, the solvent was removed under vacuum. The residue was extracted with hexane. The hexane extract was concentrated under vacuum and kept at −30 °C to give **6** (0.18 g, 0.33 mmol, 65% yield) as yellow crystals. ^{1}H NMR (400 MHz, C$_6$D$_6$, room temperature, δ/ppm): −1.25 (d, 2H, J = 11.2 Hz, CH_2Si(CH$_3$)$_3$), −1.13 (d, 2H, J = 10.8 Hz, CH_2Si(CH$_3$)$_3$), 0.15 (s, 18H, Si(CH_3)$_3$), 1.45 (s, 18H, C(CH_3)$_3$), 1.99 (s, 6H, N(CH_3)$_2$), 2.53 (t, 2H, J = 6.2 Hz, CH$_2$CH_2N(CH$_3$)$_2$), 2.80 (t, 2H, J = 6.2 Hz, −CH_2CH$_2$N(CH$_3$)$_2$), 7.28−8.20 (m, 6H, fluorenyl-H). ^{13}C NMR (100 MHz, C$_6$D$_6$): 4.0, 24.8, 31.6, 34.8, 35.9, 47.7, 67.3, 70.8, 119.4, 120.9, 124.4, 139.1, 147.3, 149.8. Anal. Calcd for C$_{33}$H$_{56}$NScSi$_2$: C, 72.36; H, 6.62; N, 2.56. Found: C, 72.48; H, 6.05; N, 2.60.

Synthesis of (2,7-^{t}Bu$_2$-9-SiMe$_3$Flu)Sc(CH$_2$SiMe$_3$)$_2$(μ-Cl)Li(THF)$_3$ (7). ScCl$_3$ (0.076 g, 0.50 mmol) was refluxed in 10 mL of THF at 100 °C for 12 h. The solution was cooled with stirring at room temperature to give a white suspension of ScCl$_3$(THF)$_3$. A THF solution (5 mL) of 2,7-^{t}Bu$_2$-9-SiMe$_3$FluLi (0.18 g, 0.50 mmol), which was prepared by the reaction of 2,7-^{t}Bu$_2$-9-SiMe$_3$Flu with n-BuLi (0.21 mL, 0.50 mmol), was added slowly and stirred at room temperature for 3.5 h. A THF solution (3 mL) of Me$_3$SiCH$_2$Li (0.094 g, 1.00 mmol) was then added slowly. After the mixture was stirred at room temperature for 30 min, the solvent was removed under vacuum. The residue was extracted with toluene. The toluene extract was concentrated under vacuum and covered with hexane at −30 °C to give **7** as colorless crystals (0.17 g, 0.20 mmol, 40% yield). ^{1}H NMR (400 MHz, C$_6$D$_6$, 22 °C, δ/ppm): −0.42 (d, 2H, J = 11.2 Hz, CH_2Si(CH$_3$)$_3$), −0.25 (s, 2H, J = 10.8 Hz, CH_2Si(CH$_3$)$_3$), 0.111 (s, 18H, CH$_2$Si(CH_3)$_3$), 0.70 (s, 9H, Si(CH_3)$_3$), 1.37 (m, 12H, THF-β-CH$_2$), 1.40 (s, 18H, C(CH_3)$_3$), 3.51 (m, 12H, THF-α-CH$_2$), 7.21−8.12 (m, 6H, fluorenyl). ^{13}C NMR (400 MHz, C$_6$D$_6$): 2.1, 4.0, 24.4, 31.4, 35.9, 46.0, 63.2, 96.0, 114.3, 116.4, 119.4, 124.3, 138.6, 147.9. Anal. Calcd for C$_{44}$H$_{79}$O$_3$ClScLiSi$_3$: C, 63.85; H, 9.62. Found: C, 63.59; H, 10.02.

Syndiospecific Polymerization of Styrene. A typical polymerization reaction is given below. In the glovebox, 2.184 g (21 mmol) of styrene was added to a toluene solution (5 mL) of Flu′Sc-(CH$_2$SiMe$_3$)$_2$(THF)$_n$ (**1**−**6**; 21 μmol) and 15 equiv of Al^{i}Bu$_3$ (315 μmol) in a 100 mL flask. The mixture was stirred at room temperature for a few minutes, during which time it turned yellow. A toluene solution (7 mL) of [Ph$_3$C][B(C$_6$F$_5$)$_4$] (19 mg, 21 μmol) was added with vigorous stirring. The magnetic stirring was ceased within a few seconds due to the viscosity. The flask was then taken outside of the glovebox. Methanol (2 mL) was added to terminate the polymerization. The mixture was poured into methanol (400 mL) to precipitate the polymer product. The white polymer powder was collected by filtration and dried under vacuum at 80 °C to a constant weight. The use of [PhMe$_2$NH][B(C$_6$F$_5$)$_4$] instead of [Ph$_3$C][B(C$_6$F$_5$)$_4$] gave similar results.

Copolymerization of Styrene with Ethylene. A typical copolymerization reaction is given below. In the glovebox, 20 mL of toluene, 2.148 g (21 mmol) of styrene, and 210 μmol of Al^{i}Bu$_3$ were put together in a 100 mL two-necked flask with a stirring bar. The flask was taken outside of the glovebox and attached to a well-purged ethylene Schlenk line with a mercury-sealed stopper. The flask was placed in a water bath at 25 °C, and ethylene was then introduced with rapid stirring. The active species generated by the reaction of 21 μmol of (Flu′)Sc(CH$_2$SiMe$_3$)$_2$(THF)$_n$, 21 μmol (19 mg) of [Ph$_3$C][B(C$_6$F$_5$)$_4$], and 105 μmol of Al^{i}Bu$_3$ in 5 mL of toluene was quickly added into the flask via a syringe. The polymerization was terminated after 2 min by addition of 2 mL of methanol. The mixture was poured into methanol (400 mL) to precipitate the copolymer. The white copolymer was collected by filtration and dried under vacuum at 80 °C to a constant weight.

The styrene contents of the copolymers were calculated from the ^{1}H NMR spectra according to the formula

$$PS\ mol\% = 4A_{ar}/(5A_{al} + A_{ar})$$

where A_{ar} = area of aromatic protons and A_{al} = area of aliphatic protons.

Solvent Extraction. All solvent fractionations were carried out using a 100 mL Soxhlet extractor. One gram of polystyrene was placed in a cellulose thimble and extracted successively with 100 mL of boiling methyl ethyl ketone (MEK) for 4 h. The residue in the thimble was dried under vacuum at 60 °C to constant weight.

X-ray Crystallographic Analysis. A crystal was sealed in oil under a microscope in the glovebox. Data collections were performed at −100 °C on a Bruker Smart-Apex CCD diffractometer with a CCD area detector using graphite-monochromated Mo Kα radiation (λ = 0.71073 Å). The determination of crystal class and unit cell parameters was carried out by the SMART program package.[16] The raw frame data were processed using SAINT[17] and SADABS[18] to yield the reflection data file. The structures were solved by using the SHELXTL-97 program.[19] Refinements were performed on F^2 anisotropically for all the non-hydrogen atoms by the full-matrix least-squares method. The analytical scattering factors for neutral atoms were used throughout the analysis. The non-hydrogen atoms were refined anisotropically. The hydrogen atoms were placed at calculated positions and were included in the structure calculations without further refinement of the parameters. The residual electron densities were of no chemical significance. Crystallographic data (excluding structure factors) have been deposited with the Cambridge Crystallographic Data Centre; supplementary publication nos. CCDC 875517 (**3**), 903048 (**4**), 875516 (**5**), 875513 (**6**), and 875514 (**7**) contain supplementary crystallographic data for this paper. These data can be obtained free of charge from The Cambridge Crystallographic Data Centre via www.ccdc.cam.ac.uk/data_request/cif.

Computational Details. The M06/6-31g(d) method[20] as well as the ONIOM[21] quantum chemistry/molecular mechanics (QM/MM) method were employed in the calculations. All of the structures involved in this study were fully optimized by considering the toluene solvation effects with the polarized continuum model (PCM).[22] The transition states were identified by having only one imaginary frequency which points to the corresponding reactants and products. All calculations were performed by utilizing the Gaussian 09 program package. Details of the computational methodology and geometries of all the structures obtained in this study are provided in the Supporting Information.

ASSOCIATED CONTENT

Ⓢ Supporting Information

Figures, tables, and a CIF file giving the geometries of all the structures obtained by DFT calculations, detailed spectra of representative polymer and copolymer products, and crystallographic data. This material is available free of charge via the Internet at http://pubs.acs.org.

AUTHOR INFORMATION

Corresponding Author

*E-mail: xfli@bit.edu.cn (X.L.); swzhang@bit.edu.cn (S.Z.); houz@riken.jp (Z.H.).

Notes

The authors declare no competing financial interest.

REFERENCES

(1) For examples: (a) Jordan, R. F.; Dasher, W. E.; Echols, S. F. *J. Am. Chem. Soc.* **1986**, *108*, 1718−1719. (b) Jordan, R. F.; Bajgur, C. S.; Willett, R.; Scott, B. *J. Am. Chem. Soc.* **1986**, *108*, 7410−7411. (c) Jordan, R. F.; Lapointe, R. E.; Bajgur, C. S.; Willett, R. *J. Am. Chem. Soc.* **1987**, *109*, 4111−4113. (d) Lin, Z.; Le Marechal, J.-F.; Sabat, M.; Marks, T. J. *J. Am. Chem. Soc.* **1987**, *109*, 4127−4129. (e) Bochmann, M.; Wilson, L. M.; Hursthouse, M. B.; Short, R. L. *Organometallics* **1987**, *6*, 2556−2563. (f) Bochmann, M.; Wilson, L. M.; Hursthouse, M. B.; Motevalli, M. *Organometallics* **1988**, *7*, 1148−1154. (g) Hlatky, G. G.; Turner, H. W.; Eckman, R. R. *J. Am. Chem. Soc.* **1989**, *111*, 2728−2729. (h) Bochmann, M.; Jaggar, A. J.; Nicholls, J. C. *Angew. Chem., Int. Ed. Engl.* **1990**, *29*, 780−782. (i) Jordan, R. F. *Adv. Organomet. Chem.* **1991**, *32*, 325−387. (j) Yang, X.; Stern, C. L.; Marks, T. J. *J. Am. Chem. Soc.* **1991**, *113*, 3623−3625. (k) Ewen, J. A.; Elder, M. J., Eur. Patent Appl. 0,427,697, 1991; U.S. Pat. 5,561,092, 1996. (l) Horton, A. D.; Frijns, J. H. G. *Angew. Chem., Int. Ed. Engl.* **1991**, *30*, 1152−1154. (m) Chien, J. C. W.; Tsai, W.-M.; Rausch, M. D. *J. Am. Chem. Soc.* **1991**, *113*, 8570−8571. (n) Yang, X.; Stern, C. L.; Marks, T. J. *Organometallics* **1991**, *10*, 840−842. (o) Hlatky, G. G.; Upton, D. J.; Turner, H. W. PCT Int. Appl. WO 91/09882 1991. (p) Siedle, A. R.; Lamanna, W. M.; Newmark, R. A.; Stevens, J.; Richardson, D. E.; Ryan, M. *Makromol. Chem., Macromol. Symp.* **1993**, *66*, 215−224. (q) Ewen, J. A.; Elder, M. J. *Makromol. Chem., Macromol. Symp.* **1993**, *66*, 179−190. (r) Yang, X.; Stern, C. L.; Marks, T. J. *J. Am. Chem. Soc.* **1994**, *116*, 10015−10031. (s) Brintzinger, H. H.; Fischer, D.; Mülhaupt, R.; Rieger, B.; Waymouth, R. *Angew. Chem., Int. Ed. Engl.* **1995**, *34*, 1143−1170. (t) Bochmann, M. *J. Chem. Soc., Dalton Trans.* **1996**, 255−270. (u) Chen, E. Y. X.; Marks, T. J. *Chem. Rev.* **2000**, *100*, 1391−1434.

(2) For examples: (a) Chien, J. C. W.; Xu, B. *Makromol. Chem., Rapid Commun.* **1993**, *14*, 109−114. (b) Tsai, W. M.; Rausch, M. D.; Chien, J. C. W. *Appl. Organomet. Chem.* **1993**, *7*, 71−74. (c) Chien, J. C. W.; Song, W.; Rausch, M. D. *J. Polym. Sci., Part A: Polym. Chem.* **1994**, *32*, 2387−2393. (d) Bochmann, M.; Sarsfield, J. *Organometallics* **1998**, *17*, 5908−5912. (e) Nomura, K.; Naga, N.; Miki, M.; Yanagi, K. *Macromolecules* **1998**, *31*, 7588−7597. (f) Carr, A. G.; Dawson, D. M.; Thornton-Pett, M.; Bochmann, M. *Organometallics* **1999**, *18*, 2933−2935. (g) Nomura, K.; Komatsu, T.; Nakamura, M.; Imanishi, Y. *J. Mol. Catal. A Chem.* **2000**, *164*, 131−135. (h) Park, J. T.; Yoon, S. C.; Bae, B.-J.; Seo, W. S.; Suh, I.-H.; Han, T. K.; Park, J. R. *Organometallics* **2000**, *19*, 1269−1276. (i) Arndt, S.; Spaniol, T. P.; Okuda, J. *Angew. Chem., Int. Ed. Engl.* **2003**, *42*, 5075−5079. (j) Nomura, K.; Fudo, A. *J. Mol. Catal. A Chem.* **2004**, *209*, 9−17. (k) Hitzbleck, J.; Okuda, J. *Z. Anorg. Allg. Chem.* **2005**, *632*, 1947−1949. (l) Hitzbleck, J.; Becherle, K.; Okuda, J.; Halbach, T.; Muelhaupt, R. *Macromol. Symp.* **2006**, *236*, 23−29. (m) Naga, N. *J. Mol. Catal. A: Chem.* **2007**, *263*, 206−211. (n) Nakajima, Y.; Hou, Z. *Organometallics* **2009**, *28*, 6861−6870. (o) Fang, X.; Li, X.; Hou, Z.; Assoud, J.; Zhao, R. *Organometallics* **2009**, *28*, 517−522. (p) Hasumi, S.; Itagaki, K.; Zhang, S.; Nomura, K. *Macromolecules* **2011**, *44*, 773−777. (q) Jian, Z.; Cui, D.; Hou, Z. *Chem. Eur. J.* **2012**, *18*, 2674−2684.

(3) For examples: (a) Bochmann, M.; Lancaster, S. J. *Angew. Chem., Int. Ed. Engl.* **1994**, *33*, 1634−1637. (b) Bochmann, M.; Lancaster, S. J. *J. Organomet. Chem.* **1995**, *497*, 55−59. (c) Tritto, I.; Donetti, R.; Sacchi, M. C.; Locatelli, P.; Zannoni, G. *Macromolecules* **1997**, *30*, 1247−1252. (d) Tritto, I.; Donetti, R.; Sacchi, M. C.; Locatelli, P.; Zannoni, G.

Macromolecules **1999**, *32*, 264−269. (e) Babushkin, D. E.; Semikolenova, N. V.; Zakharov, V. A.; Talsi, E. P. *Macromol. Chem. Phys.* **2000**, *201*, 558−567. (f) Vanka, K.; Ziegler, T. *Organometallics* **2001**, *20*, 905−913. (g) Song, F.; Cannon, R.; Bochmann, M. *J. Am. Chem. Soc.* **2003**, *125*, 7641−7653. (h) Evans, W. J.; Champagne, T.; Giarikos, D.; Ziller, J. *Chem. Commun.* **2005**, 5925−5927.

(4) (a) Kaita, S.; Hou, Z.; Wakatsuki, Y. *Macromolecules* **1999**, *32*, 9078−9079. (b) Kaita, S.; Hou, Z.; Nishiura, M.; Doi, Y. Y.; Kurazumi, J.; Horiuch, A. C.; Wakatsuki, Y. *Macromol. Rapid Commun.* **2003**, *24*, 108−184. (c) Kaita, S.; Takeguchi, Y.; Hou, Z.; Nishiura, M.; Doi, Y.; Wakatsuki, Y. *Macromolecules* **2003**, *36*, 7923−7926.

(5) Zhang, L.; Nishiura, M.; Yuki, M.; Luo, Y.; Hou, Z. *Angew. Chem., Int. Ed.* **2008**, *47*, 2642−2645.

(6) (a) Zimmermann, M.; Tornroos, K. W.; Anwander, R. *Angew. Chem., Int. Ed.* **2008**, *47*, 775−778. (b) Zimmermann, M.; Tornroos, K. W.; Sitzmann, H.; Anwander, R. *Chem. Eur. J.* **2008**, *14*, 7266−7277. (c) Dietrich, H. M.; Tornroos, K. W.; Herdtweck, E.; Anwander, R. *Organometallics* **2009**, *28*, 6739−6740. (d) Litlabo, R.; Saliu, K.; Ferguson, M. J.; McDonald, R.; Takats, J.; Anwander, R. *Organometallics* **2009**, *28*, 6750−6754. (e) Litlabo, R.; Lee, H. S.; Niemeyer, M.; Tornroos, K. W.; Anwander, R. *Dalton Trans.* **2010**, *39*, 6815−6825. (f) Dietrich, H. M.; Maichle-Mossmer, C.; Anwander, R. *Dalt. Trans.* **2010**, *39*, 5783−5785. (g) Litlabo, R.; Enders, M.; Tornroos, K. W.; Anwander, R. *Organometallics* **2010**, *29*, 2588−2595.

(7) Evans, W. J.; Champagne, T.; Giarikos, D.; Ziller, J. *Chem. Commun.* **2005**, 5925−5927.

(8) Li, S.; Miao, W.; Tang, T.; Dong, W.; Zhang, X.; Cui, D. *Organometallics* **2008**, *27*, 718−725.

(9) (a) Luo, Y.; Baldamus, J.; Hou, Z. *J. Am. Chem. Soc.* **2004**, *126*, 13910−13911. (b) Li, X.; Baldamus, J.; Hou, Z. *Angew. Chem., Int. Ed.* **2005**, *44*, 962−965. (c) Li, X.; Hou, Z. *Macromolecules* **2005**, *38*, 6767−6769. (d) Li, X.; Baldamus, J.; Nishiura, M.; Tardif, O.; Hou, Z. *Angew. Chem., Int. Ed.* **2006**, *45*, 8184−8188. (e) Hitzbleck, J.; Beckerle, K.; Okuda, J.; Halbach, T.; Muelhaupt, R. *Macromol. Symp.* **2006**, *236*, 23−29. (f) Li, X.; Nishiura, M.; Mori, K.; Mashiko, T.; Hou, Z. *Chem. Commun.* **2007**, 4137−4139. (g) Jaroschik, F.; Shima, T.; Li, X.; Mori, K.; Ricard, L.; Le Goff, X. F.; Nief, F.; Hou, Z. *Organometallics* **2007**, *26*, 5654−5660. (h) Nishiura, M.; Mashiko, T.; Hou, Z. *Chem. Commun.* **2008**, 2019−2021. (i) Yu, N.; Nishiura, M.; Li, X.; Xi, Z.; Hou, Z. *Chem. Asian J.* **2008**, *3*, 1406−1414. (j) Zhang, H.; Luo, Y.; Hou, Z. *Macromolecules* **2008**, *41*, 1064−1066. (k) Li, X.; Nishiura, M.; Hu, L.; Mori, K.; Hou, Z. *J. Am. Chem. Soc.* **2009**, *131*, 13870−13882. (l) Xu, X.; Cheng, Y.; Sun, J. *Chem. Eur. J.* **2009**, *15*, 846−850. (m) Fang, X.; Li, X.; Hou, Z.; Assoud, J.; Zhao, R. *Organometallics* **2009**, *28*, 517−522. (n) Xu, X.; Chen, Y.; Sun, J. *Chem. Eur. J.* **2009**, *15*, 846−850. (o) Pan, L.; Zhang, K.; Nishiura, M.; Hou, Z. *Macromolecules* **2010**, *43*, 9591−9593. (p) Pan, L.; Zhang, K.; Nishiura, M.; Hou, Z. *Angew. Chem., Int. Ed.* **2011**, *50*, 12012−12015. (q) Guo, F.; Nishiura, M.; Koshino, H.; Hou, Z. *Macromolecules* **2011**, *44*, 2400−2403. (r) Guo, F.; Nishiura, M.; Koshino, H.; Hou, Z. *Macromolecules* **2011**, *44*, 6335−6344. (s) Nishiura, M.; Hou, Z. *Nat. Chem.* **2010**, *2*, 257−268.

(10) (a) Hitzbleck, J.; Beckerle, K.; Okuda, J.; Halbach, T.; Muelhaupt, R. *Macromol. Symp.* **2006**, *236*, 23−29. (b) Tritto, I.; Boggioni, L.; Ravasio, A.; Zampa, C.; Hitzbleck, J.; Okuda, J.; Bredeau, S.; Dubois, P. *Macromol. Symp.* **2007**, *260*, 114−121. (c) Hitzbleck, J.; Beckerle, K.; Okuda, J. *J. Organomet. Chem.* **2007**, *692*, 4702−4707. (d) Kramer, M.; Robert, D.; Nakajima, Y.; Englert, U.; Spaniol, T.; Okuda, J. *Eur. J. Inorg. Chem.* **2007**, *5*, 665−674. (e) Ravasio, A.; Zampa, C.; Boggioni, L.; Tritto, I.; Hitzbleck, J.; Okuda, J. *Macromolecules* **2008**, *41*, 9565−9569. (f) Ravasio, A.; Boggioni, L.; Tritto, I.; D'Arrigo, C.; Perico, A.; Hitzbleck, J.; Okuda, J. *J. Polym. Sci., Part A: Polym. Chem.* **2009**, *47*, 5709−5719. (g) Tritto, I.; Ravasio, A.; Boggioni, L.; Bertini, F.; Hitzbleck, J.; Okuda, J. *Macromol. Chem. Phys.* **2010**, *211*, 897−904.

(11) A portion of this work was reported at the 2011 Polymer Symposium of China Dalin: , Li, X.; Xu, Q.; Chen, Y. A-O-20.

(12) Shapiro, P. J.; Bunel, E. E.; Schaefer, W. P.; Bercaw, J. E. *Organometallics* **1990**, *9*, 867−869.

(13) The ^{1}H NMR spectroscopy of the reaction mixture of complex **3** and 1 equiv of Al^{i}Bu$_3$ (1.1 M solution in toluene) in C$_6$D$_6$ at room temperature showed that THF resonances shifted from δ 3.18 to δ 3.35 for α-H and from δ 1.04 to δ 0.98 for β-H, respectively. At the same time, the doublet CH$_2$ signals of Al^{i}Bu$_3$ changed from δ 0.27 to δ 0.32 and the doublet CH$_3$ signals of Al^{i}Bu$_3$ at δ 1.03 divided into three doublet signals at δ 0.86, 1.23, and 1.26. These results demonstrated the formation of Al^{i}Bu$_3$(THF).

(14) Luo, Y.; Luo, Y.; Qu, J.; Hou, Z. *Organometallics* **2011**, *30*, 2908−2919.

(15) (a) Peter, J.; Jürgen, D. *Synthesis* **1993**, 684. (b) Krutko, D. P.; Borzov, M. V.; Veksler, E. N.; Kirsanov, R. S.; Churakov, A. V. *Eur. J. Inorg. Chem.* **1999**, 1973−1979.

(16) *SMART Software Users Guide, version 4.21*; Bruker AXS, Inc.: Madison, WI, 1997.

(17) *SAINT+, Version 6.02*; Bruker AXS, Inc., Madison, WI, 1999.

(18) Sheldrick, G. M. *SADABS*; Bruker AXS, Inc., Madison, WI, 1998.

(19) Sheldrick, G. M. SHELXTL, Version 5.1; Bruker AXS, Inc.: Madison, WI, 1998.

(20) (a) Zhao, Y.; Truhlar, D. G. *Acc. Chem. Res.* **2008**, *41*, 157−167. (b) Zhao, Y.; Truhlar, D. G. *Theor. Chem. Acc.* **2008**, *120*, 215−241.

(21) Dapprich, S.; Komáromi, I.; Byun, K. S.; Morokuma, K.; Frisch, M. J. *J. Mol. Struct. (THEOCHEM)* **1999**, *462*, 1−21.

(22) Tomasi, J.; Mennucci, B.; Cammi, R. *Chem. Rev.* **2005**, *105*, 2999−3093.